

丰质子核奇异衰变和近垒奇特核反应

林承健

cjlin@ciae.ac.cn

中国原子能科学研究院核物理所，北京275信箱10分箱，102413



报告内容

一、前言

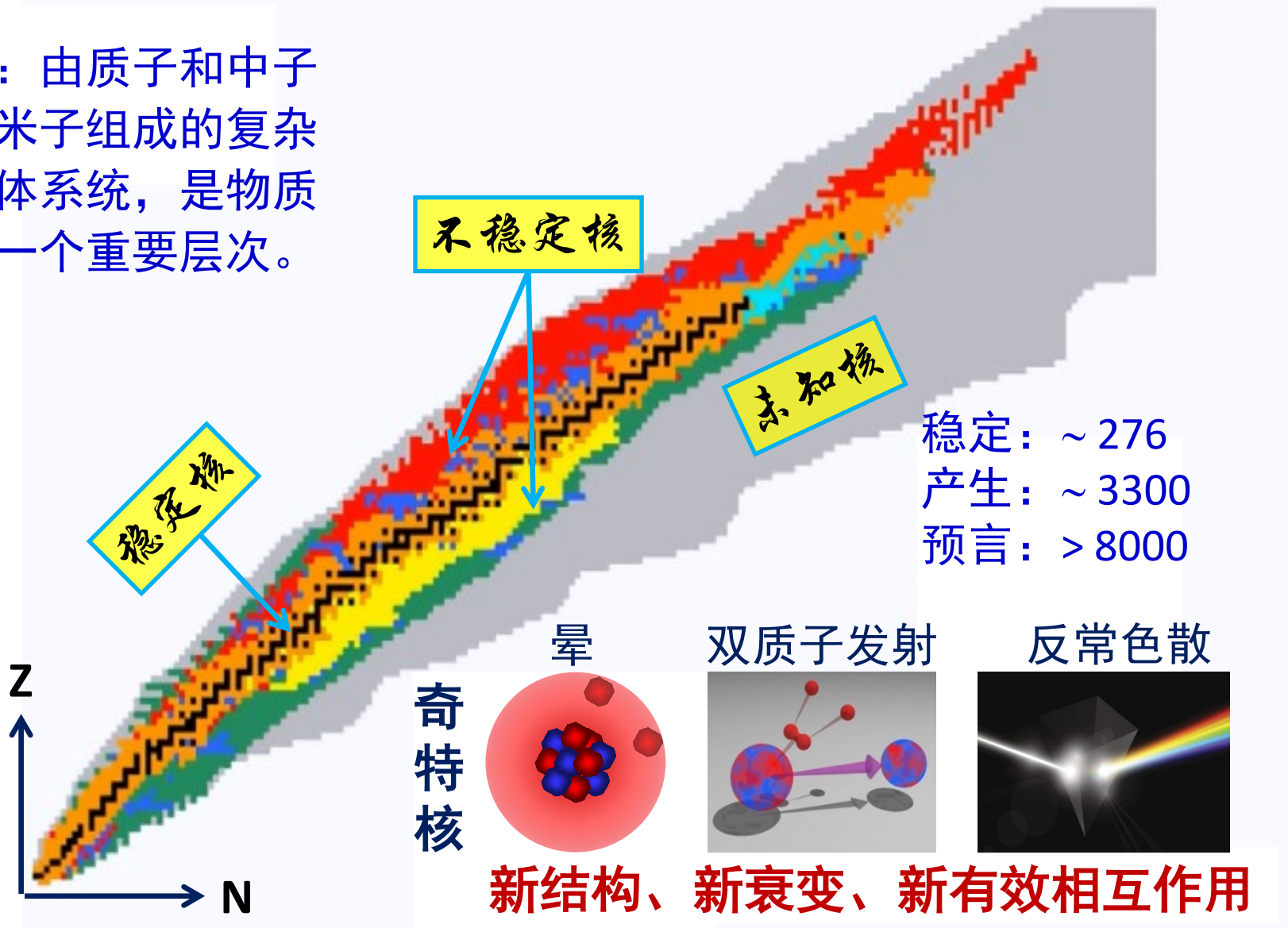
二、极丰质子核的奇异衰变

三、奇特核的近垒反应机制

四、小结

放射性核束(RIB)物理

原子核：由质子和中子两种费米子组成的复杂量子多体系统，是物质结构的一个重要层次。



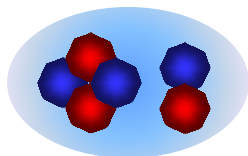
奇特核

★ Exotic nuclei:

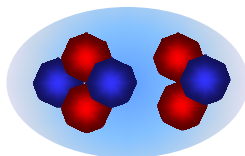
weakly-bound & having unusual structure (cluster, halo/skin ...)

Beyond the Mean Field

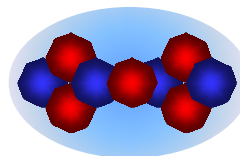
cluster



${}^6\text{Li} (\alpha+d)$
 $S_\alpha = 1.47 \text{ MeV}$

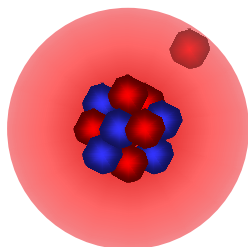


${}^7\text{Li} (\alpha+t)$
 $S_\alpha = 2.47 \text{ MeV}$

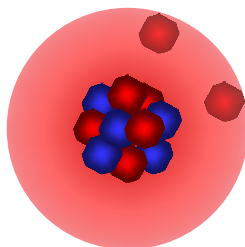


${}^9\text{Be} (\alpha+n+\alpha)$
 $S_n = 1.66 \text{ MeV}$

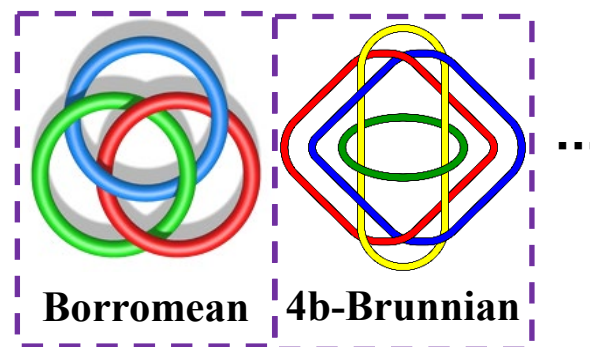
halo



${}^{11}\text{Be} ({}^{10}\text{Be}+n)$
 $S_n = 0.50 \text{ MeV}$



${}^6\text{He} (\alpha+2n)$
 $S_{2n} = 0.98 \text{ MeV}$



Borromean 4b-Brunnian

${}^{10}\text{C} (\alpha+\alpha+p+p)$

奇特核产生是一种近阈(接近分离阈)行为, 弱束缚是产生奇特结构的**首要**条件。

我国核物理实验基地

低能



HI-13串列加速器 (87)
 $(1+q)\times 13$ MeV, H-U

中能



SSC回旋加速器 (88)
100 MeV/u, C-U

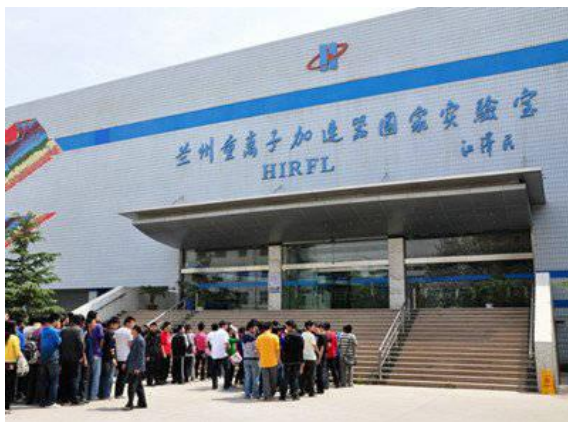
高能



正负电子对撞机 (88)
5 GeV, e^+e^-



北京串列加速器
国家实验室(BTANL)



兰州重离子加速器
国家实验室(HIRFL)

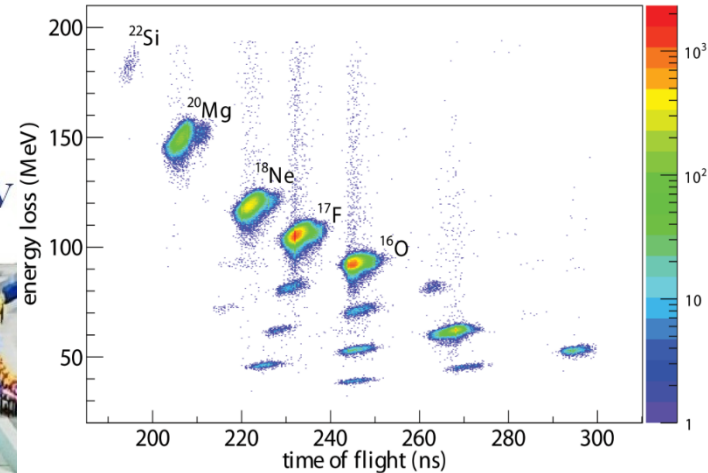


北京正负电子对撞机
国家实验室(BEPC)

放射性核束的产生：PF法

SSC (K=450)
100 AMeV (H.I.), 110 MeV (p)

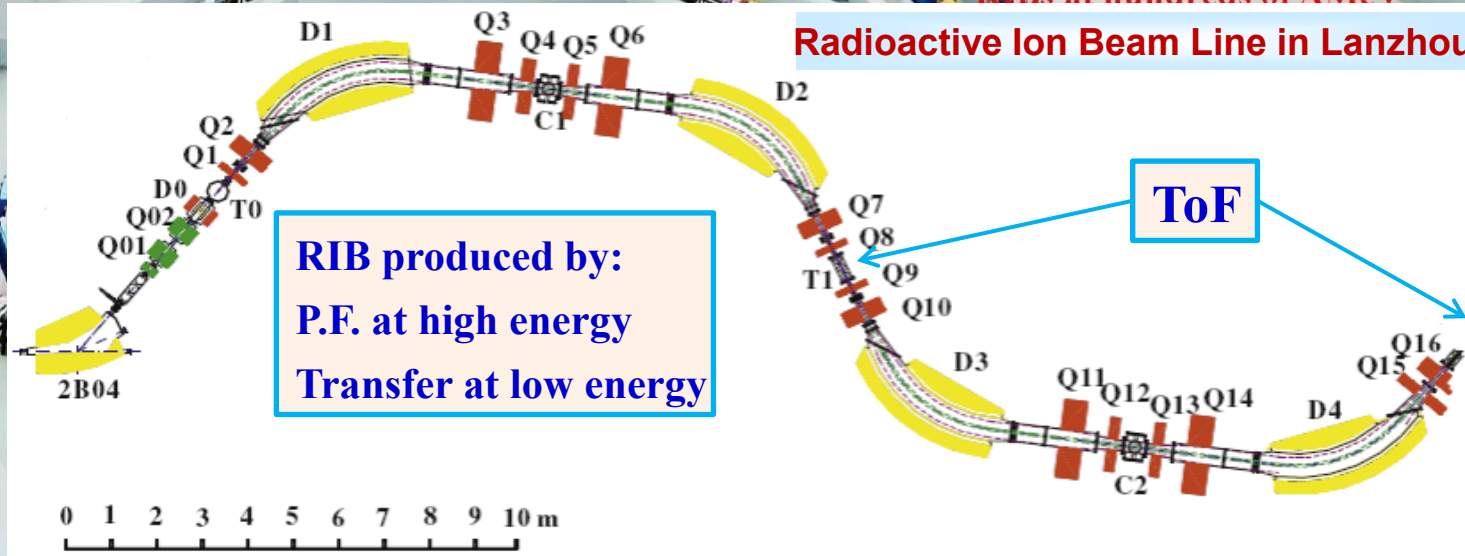
SFC (K=69)
10 AMeV (H.I.), 17~35 MeV



RIBLL1

RIBs at tens of AMeV

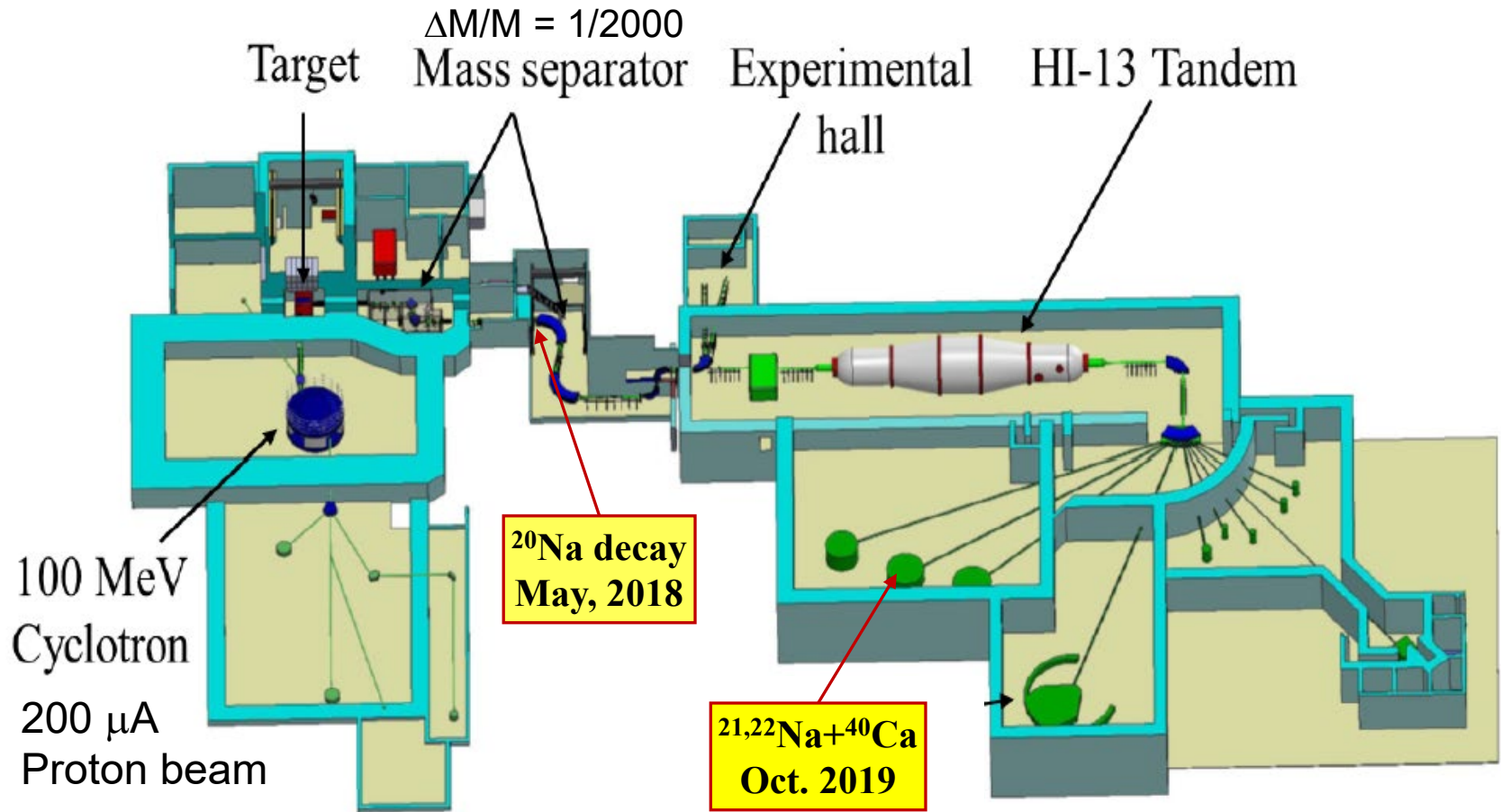
Radioactive Ion Beam Line in Lanzhou



Heavy Ion Research Facility in Lanzhou (HIRFL)

放射性核束的产生：ISOL法

Beijing Radioactive Ion-beam Facility (BRIF)



报告内容

一、前言

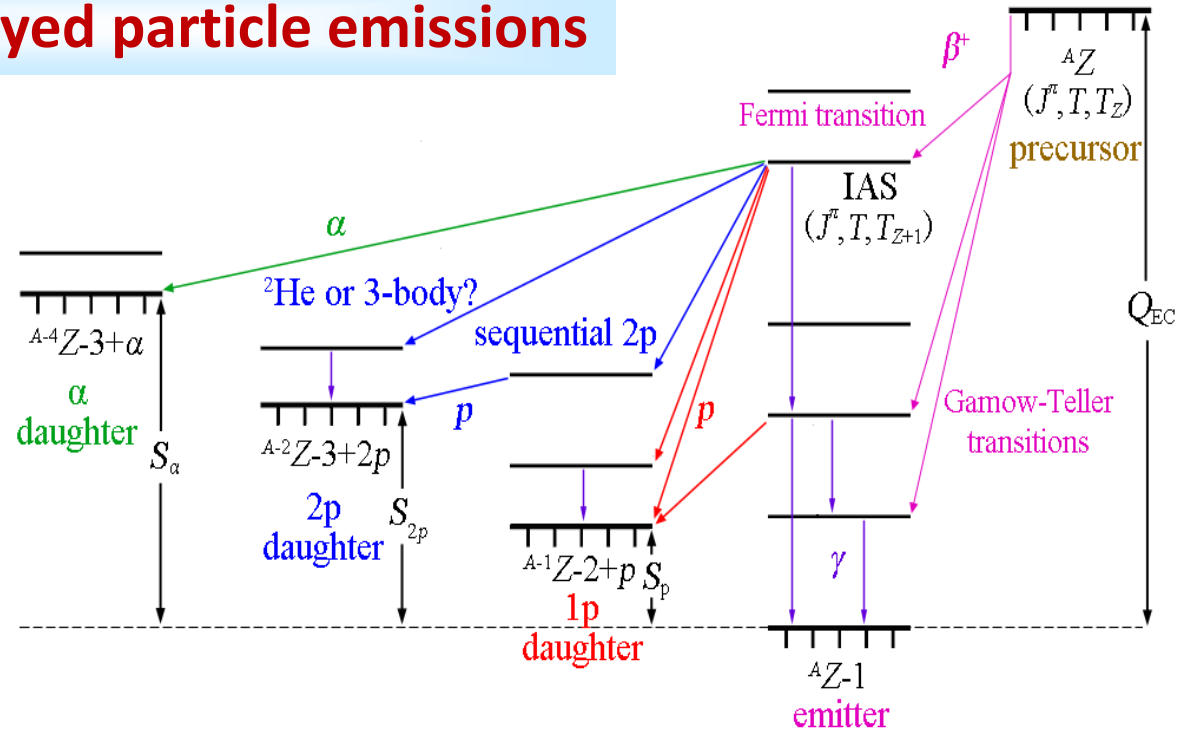
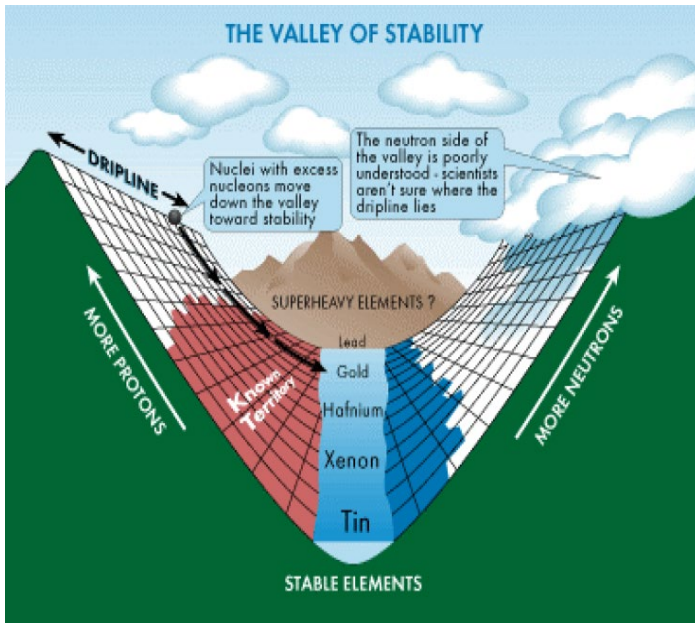
二、极丰质子核的奇异衰变

三、奇特核的近垒反应机制

四、小结

极丰质子核的奇异衰变

Beta-delayed particle emissions



$\beta p, \beta 2p, \beta 3p, \beta p\gamma, \beta\gamma p, \beta\alpha, \beta 2\alpha, \beta\alpha p, \beta p\alpha, \beta p 2\alpha, \beta n, \beta 2n, \beta 3n, \beta d, \beta t, \beta F \dots$

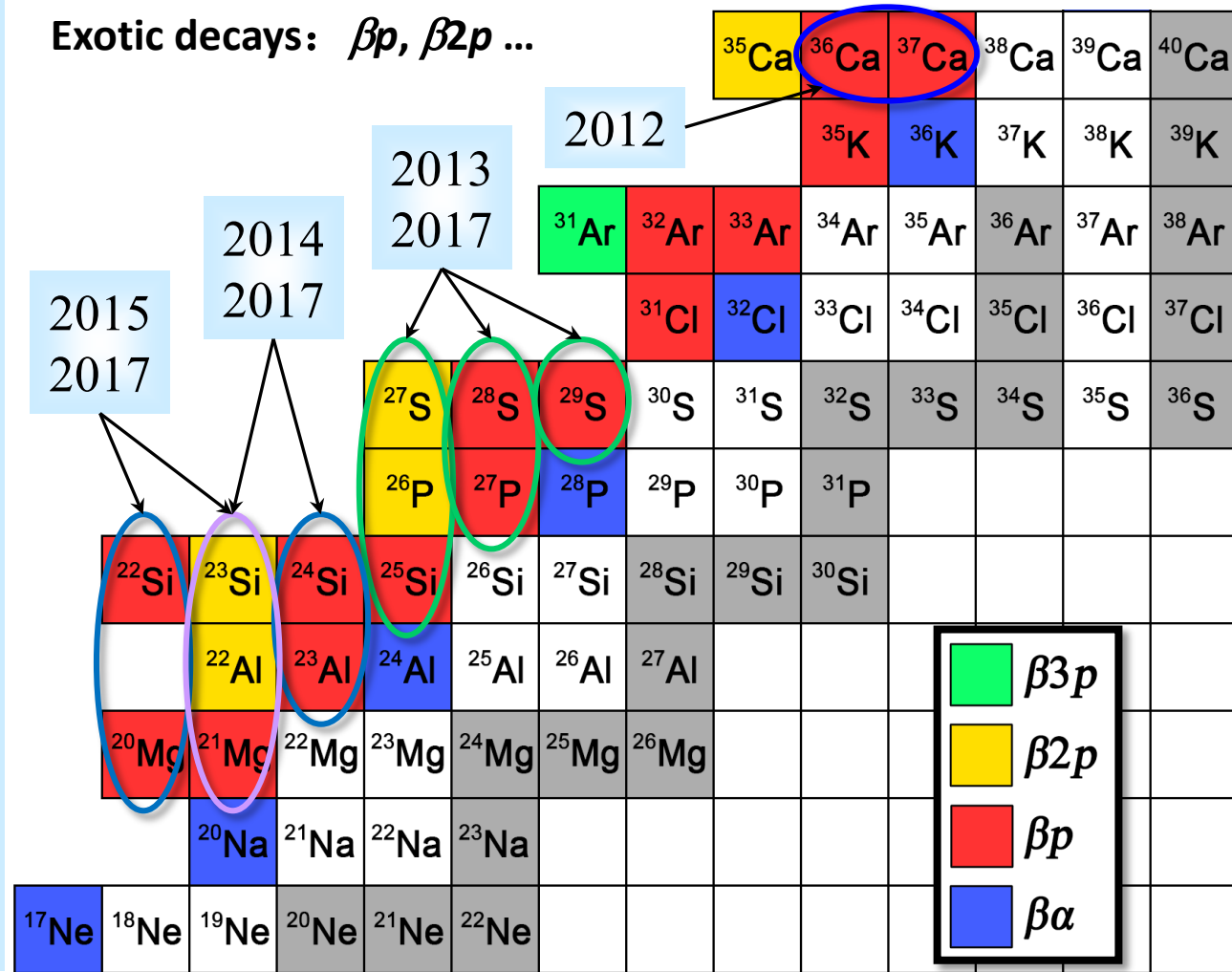
- Structures of p -rich nuclei close to/beyond the drip-line
- Effective interaction – pairing, isospin non-conserving (INC), three-body force
- Initial state interaction (ISI), final state interaction (FSI), quantum entanglement
- Nuclear astrophysics – $(p, \gamma), (2p, \gamma), (\alpha, \gamma) \dots$ processes

sd壳层丰质子核的衰变

β -decay spectroscopy of nuclei close to the proton drip line

$^{36,37}\text{Ca}$: CPL **32**, 012301 (2015);
 ^{28}S : NPR **38**, 117 (2021);
 ^{27}S : PRC **99**, 064312 (2019);
 PLB **802**, 135213 (2020);
 PRC **103**, L061301 (2021);
 ^{26}P : PRC **101**, 024305 (2020);
 Sym. **13**, 2278 (2021);
 ^{23}Al , ^{24}Si : NIMA **804**, 1 (2015);
 ^{22}Si : PLB **766**, 321 (2017);
 PRL **125**, 192503 (2020);
 ^{20}Mg : PRC **95**, 014314 (2017);
 ^{23}Si : IJMPE **27**, 1850014 (2018);
 ^{22}Al : NST **29**, 98 (2018);
 PLB **784**, 12 (2018);
 PRC **104**, 044311 (2021);
 ^{21}Mg : EPJA **54**, 107 (2018);
 ...

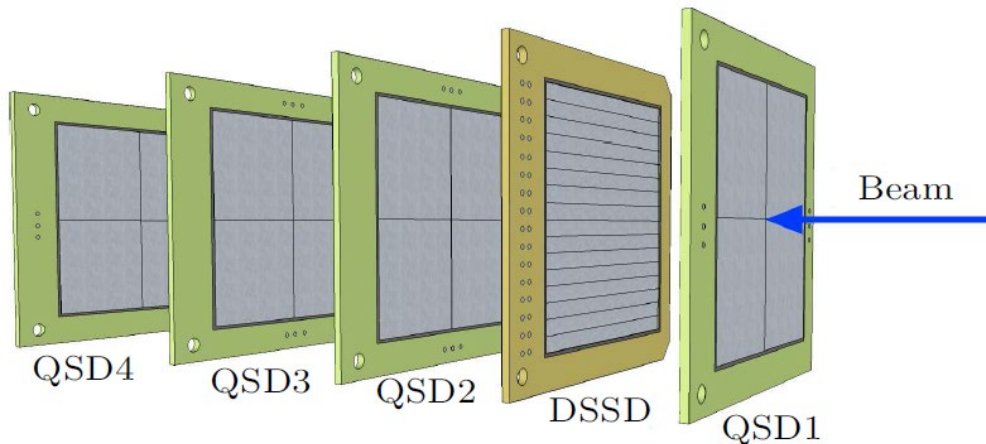
Exotic decays: βp , $\beta 2p$...



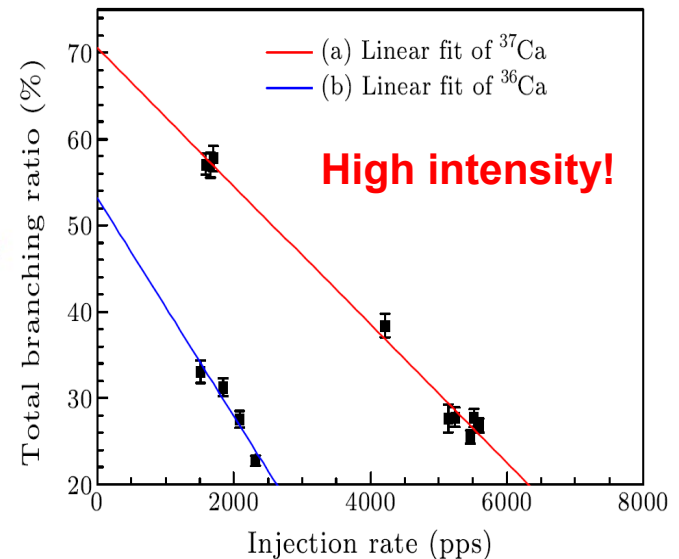
Detection Method

Test of the continuous-beam mode

- Beam on/off: implant (0.1 ms) - decay measure (> 1000 ms)
low efficiency ☹️, low background 😊;
- Continuous beam: implant & decay, time & position correlated measure
high efficiency 😊, high background ☹️ → coincident measurement 😊



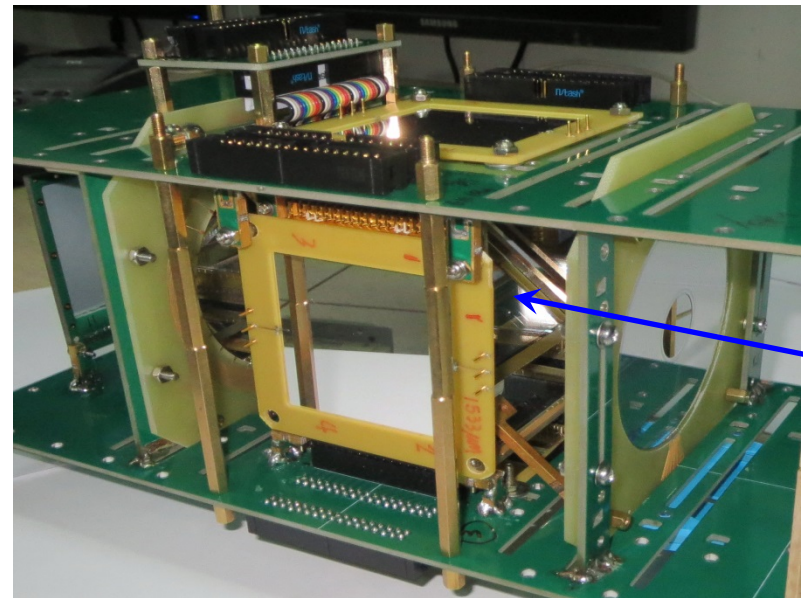
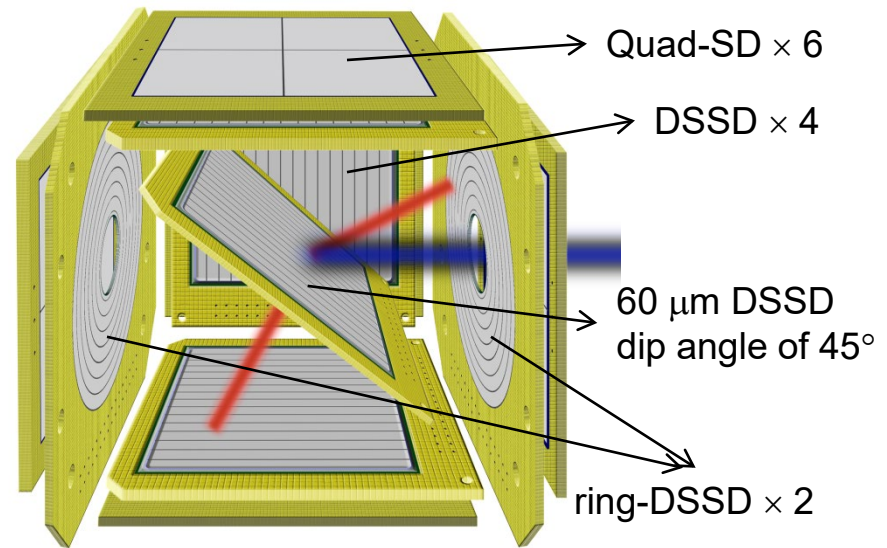
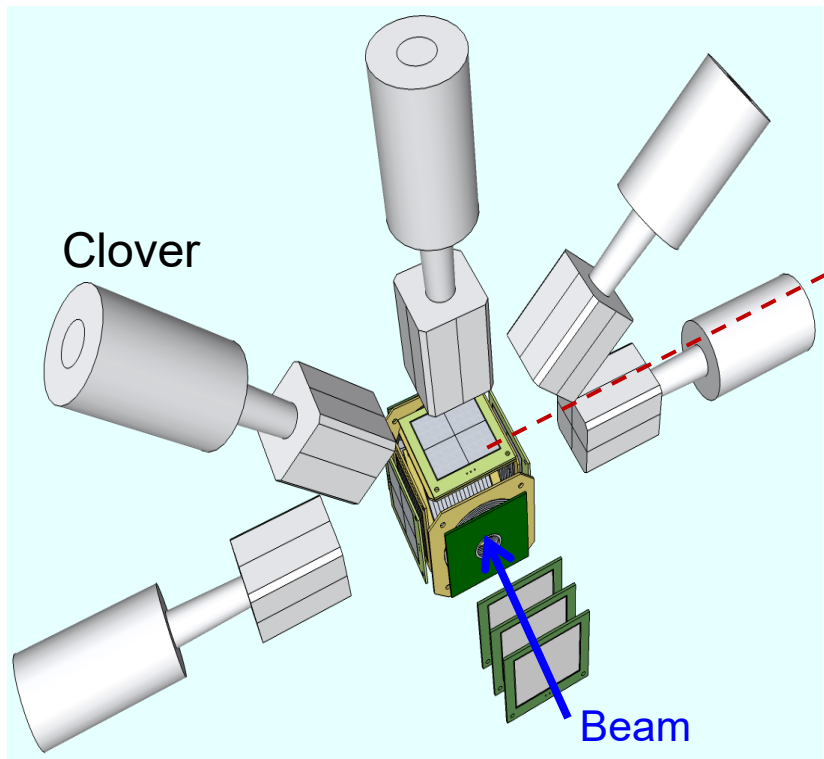
Layout of the detection setup



$^{36,37}\text{Ca}$ βp decay energies, half-lives and branching-ratios have been confirmed.

Sun Li-Jie, LIN Cheng-Jian*, Xu Xin-Xing *et al.*, Chin. Phys. Lett. **32**, 012301 (2015).

Detector Array – G1

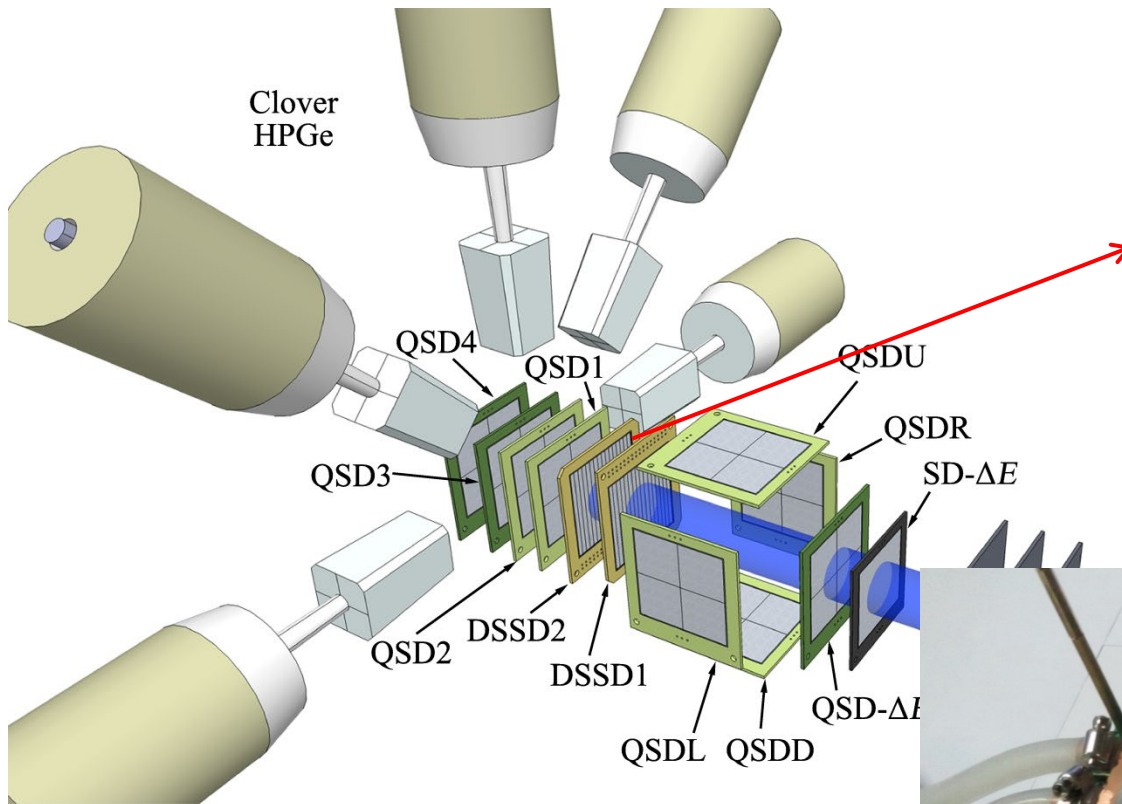


A detector array for $2p$ -decay study
by **implantation** method

for lifetime $> 10 \mu$ s

1p efficiency: $\sim 65\%$; 2p efficiency: $\sim 20\%$

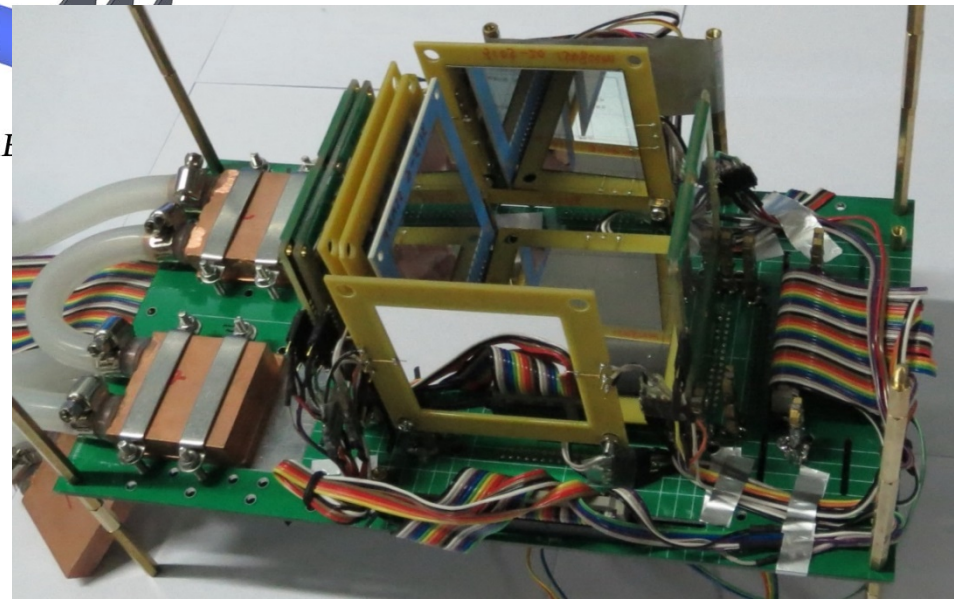
Detector Array – G2



- 150 μm + 60 μm DSSDs for ion implantations and $p/2p$ -decay measurements.
- Others for β -decay measu. and background rejection.

L.J. Sun *et al.*, NIMA **804**, 1 (2015).

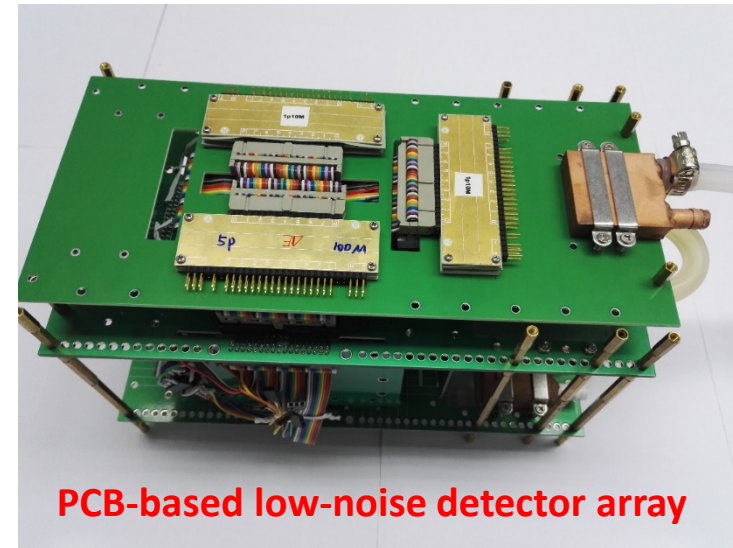
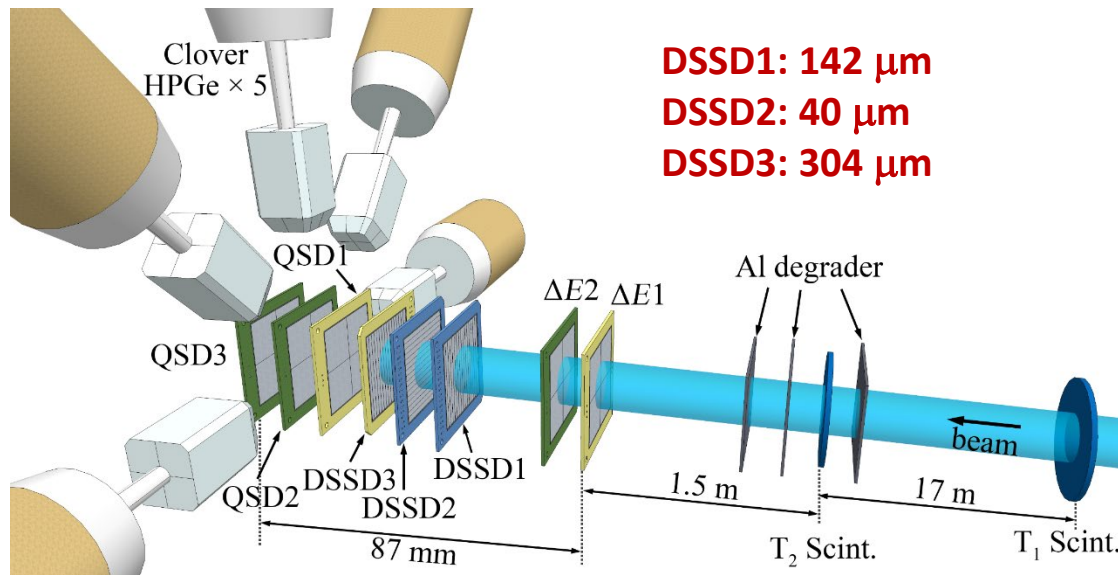
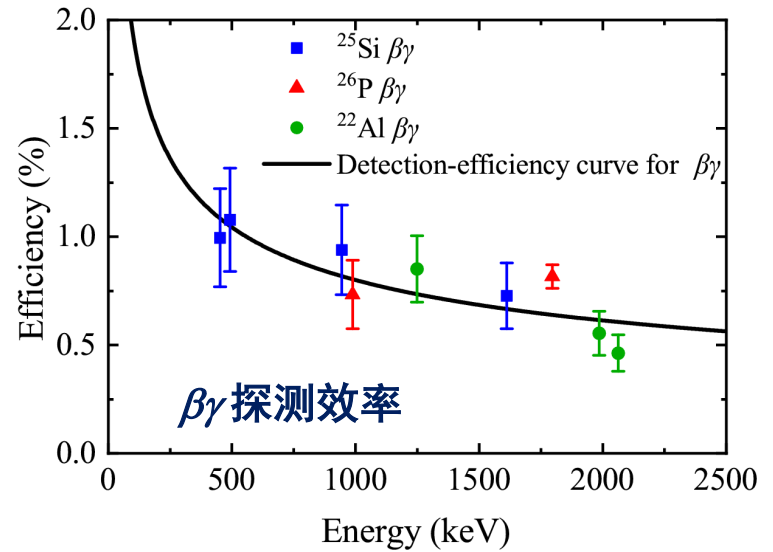
- ♣ Implanted close to the back edge of the 150 μm DSSD.
- ♣ 1p efficiency: $\sim 70\%$;
2p efficiency: $\sim 20\%$



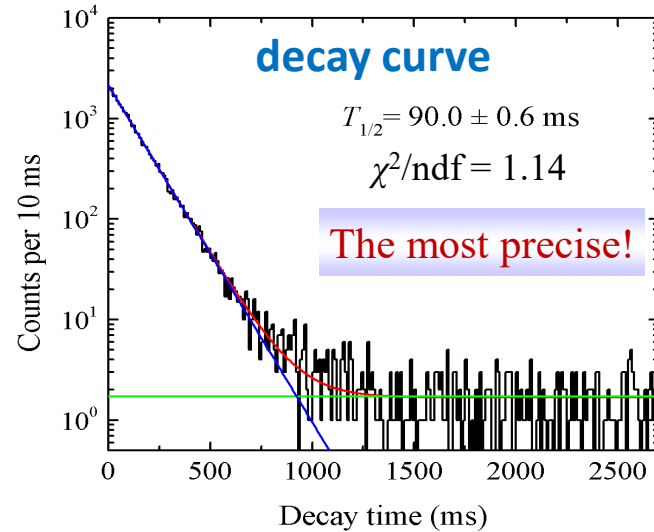
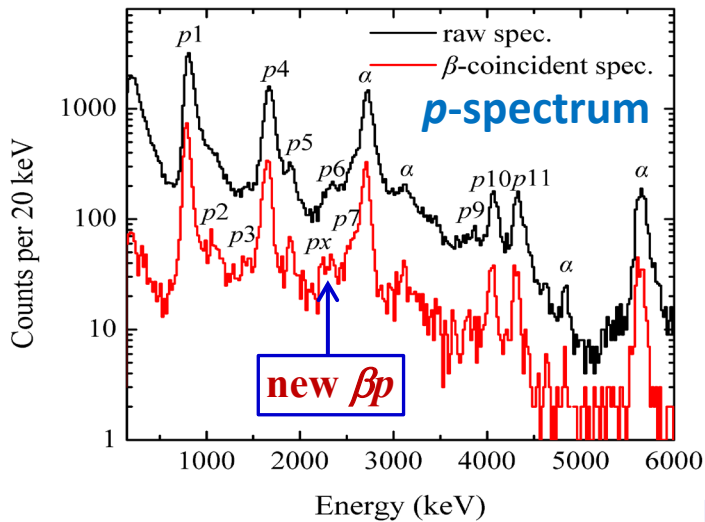
Detector Array – G3

阻停-衰变探测器阵列:

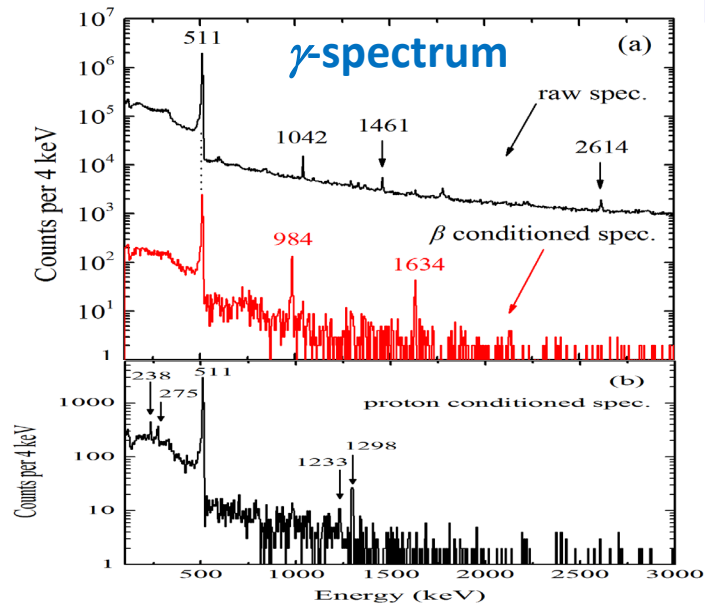
- 连续束注入-衰变探测方法，高精度 β 延迟质子/双质子衰变谱学与衰变机制研究。
- 厚薄DSSD组合，兼顾能量分辨和探测效率。
- 高探测效率： $\sim 50\%$ (1p)； $\sim 15\%$ (2p)
低探测阈值： ~ 200 keV； ~ 100 keV (数字化)
高能量分辨： < 35 keV； ~ 20 keV (数字化)



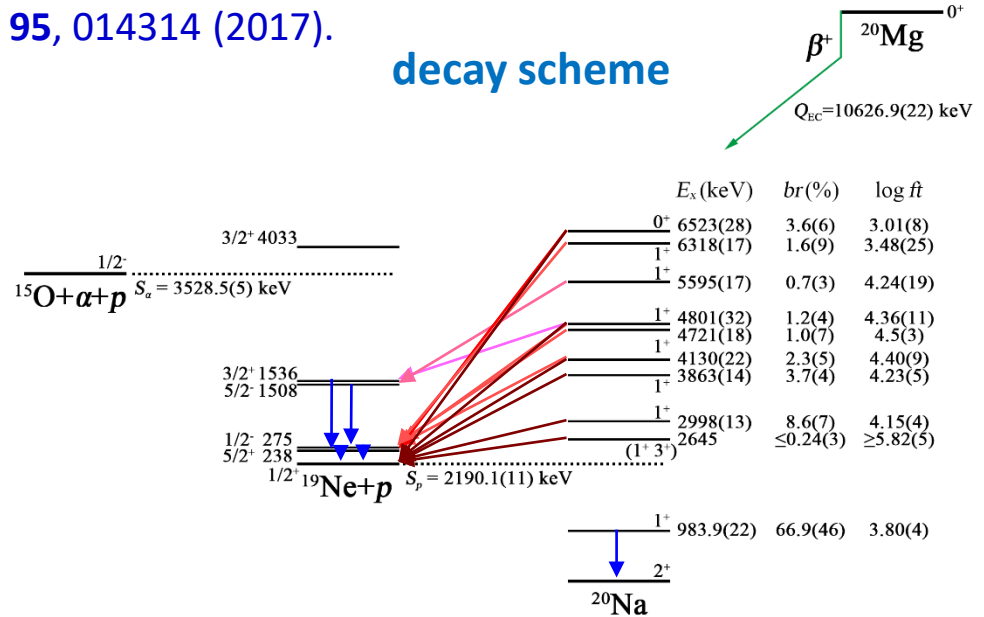
^{20}Mg Decays



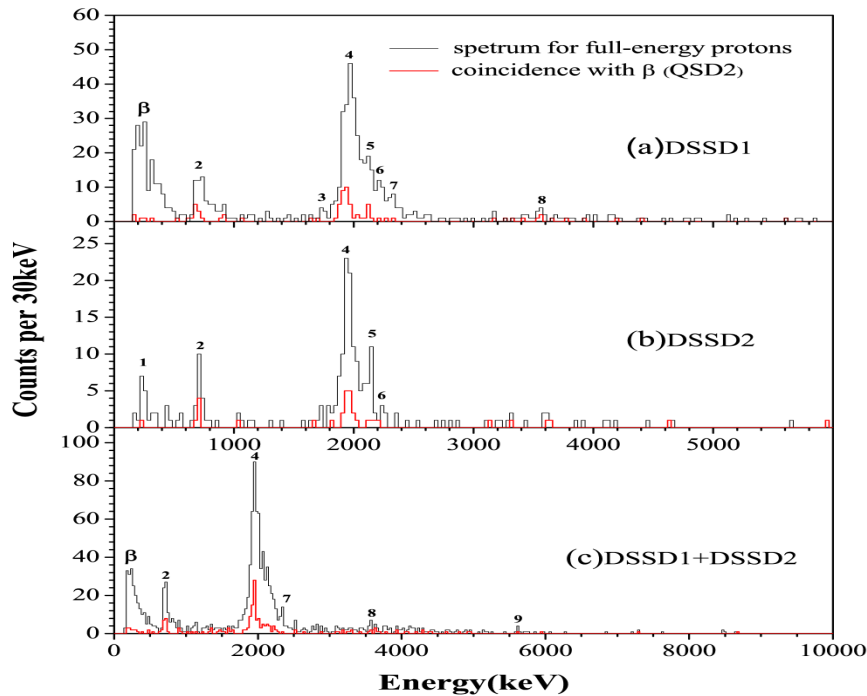
L. J. Sun et al.,
PRC 95, 014314 (2017).



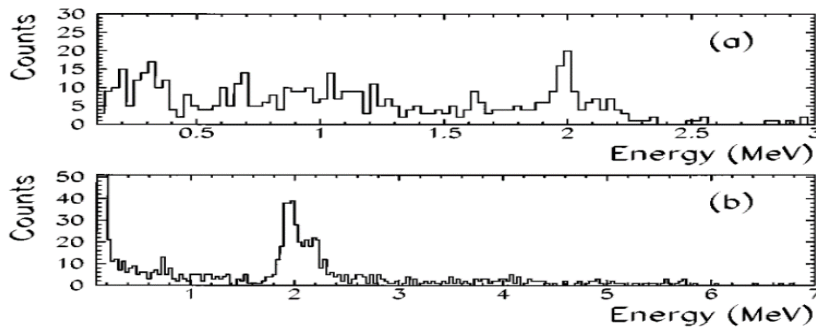
decay scheme



^{22}Si Decays



CIAE - Phys. Lett. B 766, 312 (2017).



GANIL - Phys. Rev. Lett. 59, 33 (1987).
Phys. Rev. C 54, 572 (1996).

Peak	Energy (keV)	BR (%)	Decay Mode
1	230(50)	2.9(10)	$2p$?
2	680(50)	6.8(14)	βp
3	1710(50)	1.9(7)	βp
4	1950(50)	52.0(74)	βp
5	2110(50)	10.9(21)	βp
6	2180(50)	6.5(15)	βp
7	2330(50)	5.1(13)	βp
8	3550(50)	2.5(9)	βp
9	5600(70)	0.7(3)	$\beta 2p$

★ ^{22}Si is a precursor of $\beta 2p$ decay.

★ Mass of ^{22}Si

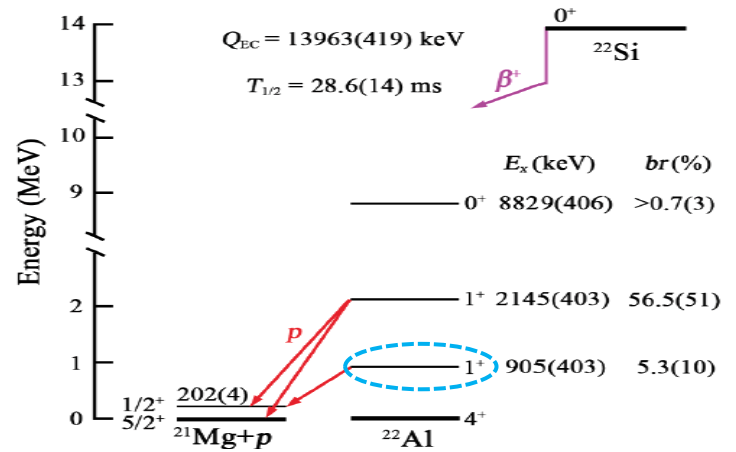
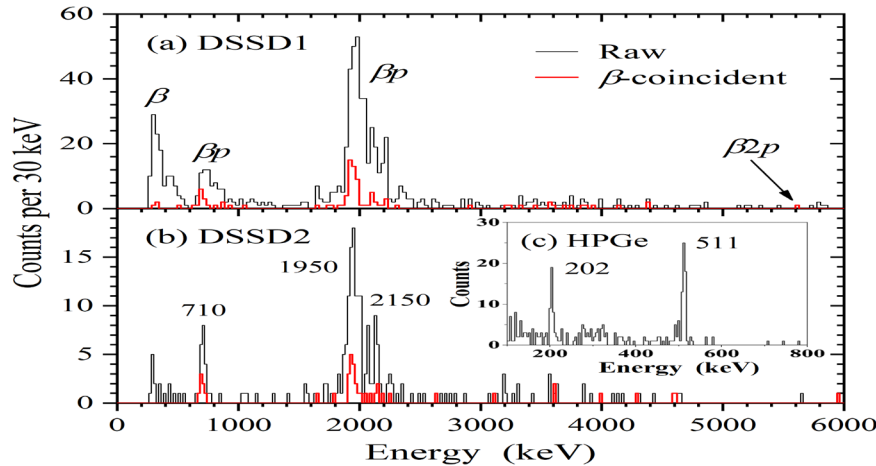
- $\Delta(^{22}\text{Si}) = \Delta(^{22}\text{Al IAS}) + \Delta E_C - \Delta_{nH}$

- $\rightarrow S_{2p} = -108 \pm 125 \text{ keV};$

- $\Delta(^{22}\text{Si}) = \Delta(^{22}\text{O}) - 2b(A, T)T_Z$

- $\rightarrow S_{2p} = -15 \text{ keV}$

Exotic Decays of ^{22}Si



★ 首次发现 ^{22}Si 存在 $\beta 2p$ 衰变模式，由此给出其实验质量，表明它是一个非常边缘的核，三体力扮演了重要作用。
X.X. Xu *et al.*, PLB 766, 312 (2017).

表： $^{22}\text{Si}/^{22}\text{O}$ 衰变的比较

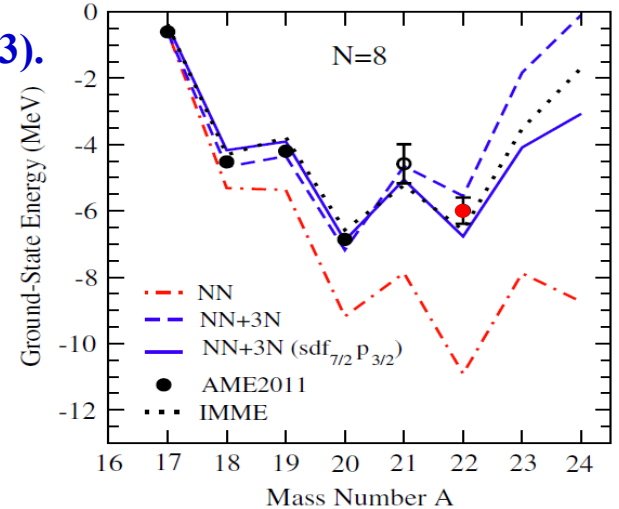
$^{22}\text{Si} \rightarrow ^{22}\text{Al} \quad Q_{\text{EC}} = 13963 \text{ keV}$					$^{22}\text{O} \rightarrow ^{22}\text{F} \quad Q_{\beta^-} = 6490 \text{ keV}$					$\delta = \frac{ft^+}{ft^-} - 1$		
Experiment			Calculations		Experiment			Calculations		δ (%)		
I_i^π	E_x (MeV)	$br\%$	$\log(ft^+)$	E_x (MeV)	$\log(ft^+)$	E_x (MeV)	$br\%$	$\log(ft^-)$	E_x (MeV)	$\log(ft^-)$	Experiment	Calculations
1_1^+	0.905	5.3 (10)	5.09 (9)	1.12 [1.69]	4.81 [4.52]	1.625	29 (4)	4.6 (1)	1.98 [1.56]	4.32 [4.56]	209 (96)	212 [-7]
1_2^+	2.145	56.5 (51)	3.83 (5)	2.43 [2.55]	3.71 [3.72]	2.572	68 (6)	3.8 (1)	2.58 [2.51]	3.72 [3.68]	7 (28)	-3.4 [10]

★ 在镜像核 $^{22}\text{Si}/^{22}\text{O}$ 衰变中发现一个极大的同位旋不对称性($\delta \sim 209\%$)，包含同位旋不守恒力的壳模型计算重现了实验结果，指出这个大的不对称性来源于 $^{22}\text{Al} \ s_{1/2}$ 轨道的晕结构。
J. Lee *et al.*, PRL 125, 192503 (2020).

Discussions on $^{22}\text{Si}/^{20}\text{Mg}$

☞ **Mass → Three-Body Force** [PRL110,022502\(2013\)](#).

Nucleus	Expt. [IMME]	S_p $NN + 3N$		Expt. [IMME]	S_{2p} $NN + 3N$	
		sd	$sdf_{7/2}P_{3/2}$		sd	$sdf_{7/2}P_{3/2}$
^{18}Ne	3.92	4.05	3.76	4.52	4.67	4.17
^{19}Na	-0.32	-0.32	-0.26	3.60	3.73	3.50
^{20}Mg	2.66	2.83	2.98	2.34	2.51	2.72
^{21}Al	[-1.34]	-2.52	-1.83	[1.45]	0.30	1.15
^{22}Si	[1.35]	0.90	1.71	[0.01]	-1.63	-0.12



(Isospin Non-Conservation)

☞ **Mirror asymmetry → INC interaction** asymmetry parameter: $\delta = \frac{ft^+}{ft^-} - 1$

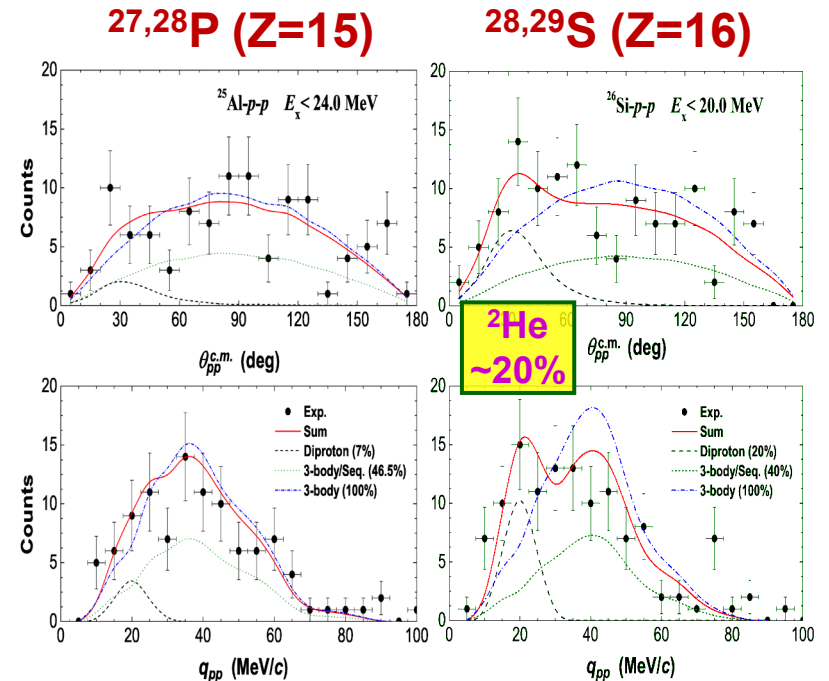
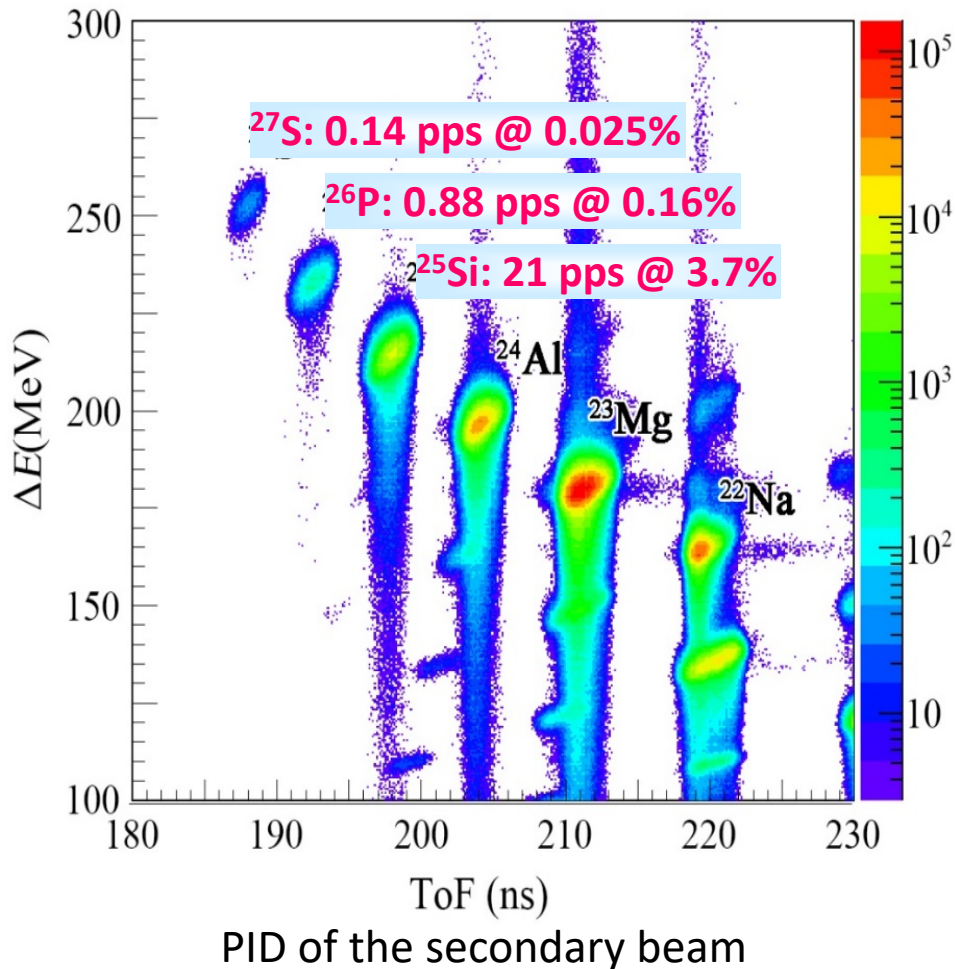
$^{20}\text{Mg} \rightarrow ^{20}\text{Na}$				$^{20}\text{O} \rightarrow ^{20}\text{F}$			
$^{20}\text{Na} E^*$ (keV)	br (%)	$\log ft$	J^π	$^{20}\text{F} E^*$ (keV)	br (%)	$\log ft$	δ
983.9(22)	66.9(46)	3.80(4)	1^+	1056.848(4)	99.973(3)	3.740(6)	0.148(107)
2998(13)	8.6(7)	4.15(4)	1^+	3488.54(10)	0.027(3)	3.65(6)	2.16(53)
$^{22}\text{Si} \rightarrow ^{22}\text{Al}$				$^{22}\text{O} \rightarrow ^{22}\text{F}$			
$^{22}\text{Al} E^*$ (keV)	br (%)	$\log ft$	J^π	$^{22}\text{F} E^*$ (keV)	br (%)	$\log ft$	δ
1170(50)	5.1(3)	5.10(5)	1^+	1625	29(4)	4.6(1)	2.16(82)
2400(50)	60.6(65)	3.79(7)	1^+	2572	68(6)	3.8(1)	-0.02(28)

PRC **95**,
014314
(2017).

PRL **125**,
192503
(2020).

Results2: $^{27}\text{S}/^{26}\text{P}$ Cases

Primary beam: ^{32}S , 80.6 MeV/u @ 90 enA.



★ Diproton emissions from the excited states of $^{28,29}\text{S}$, but none for $^{27,28}\text{P}$.

$^{28}\text{S}/^{27}\text{P}$: Phys. Lett. B **727**, 126 (2013).

^{29}S : Phys. Rev. C **80**, 014310 (2009);

^{28}P : PRC **81**, 054317 (2010).

^{27}S Decays

27 βp & 1 $\beta 2p$ decays

Old: p_1, p_2, p_{10} (BR>5.7%)

New: 24 βp (BR>0.3%) & 1 $\beta 2p$

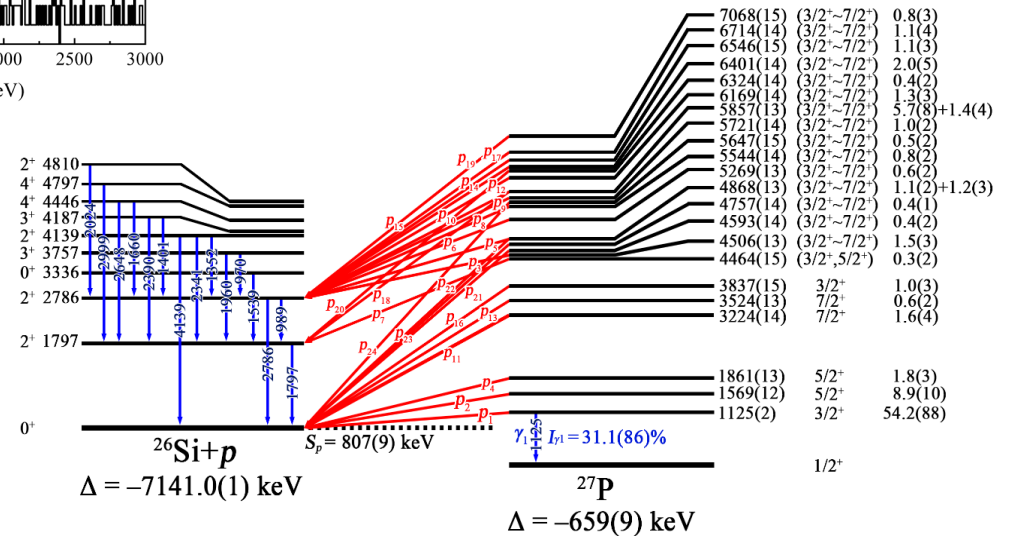
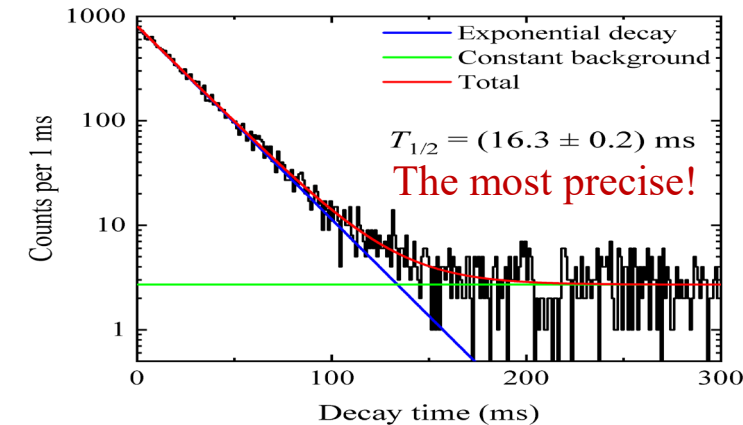
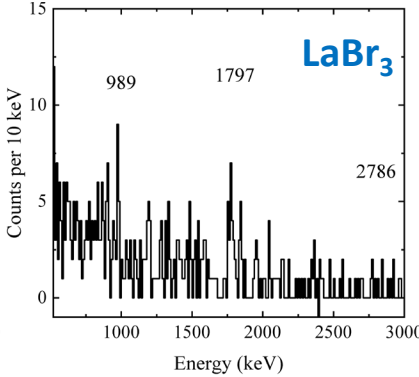
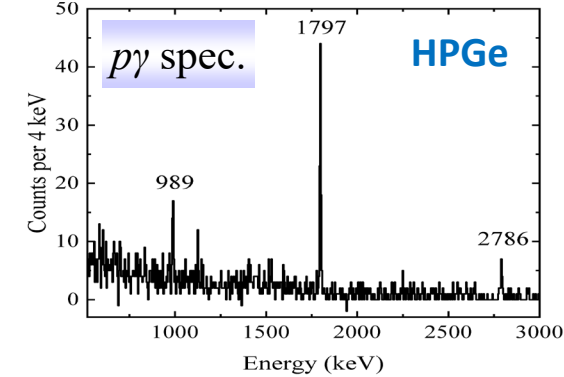
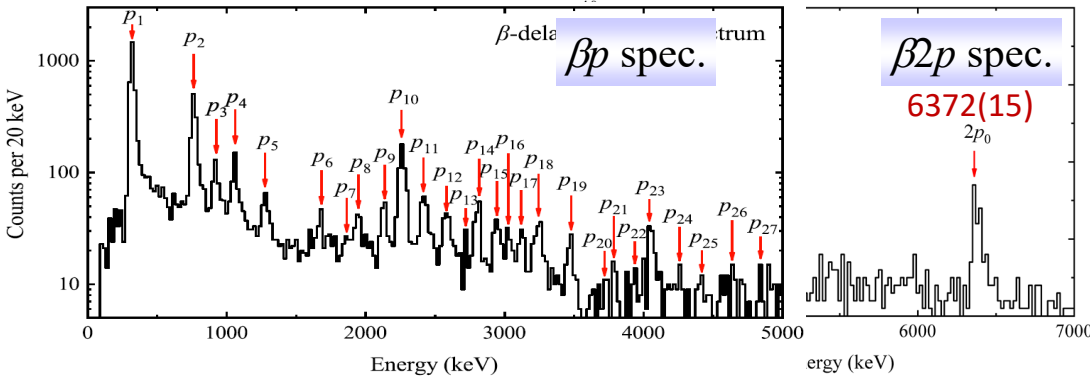
$T_{1/2} = 16.3(2)$ ms $T = 2$

^{27}S $5/2^+$
 β^+ $\Delta = 17678(77)$ keV

$Q_{EC} = 18337(78)$ keV

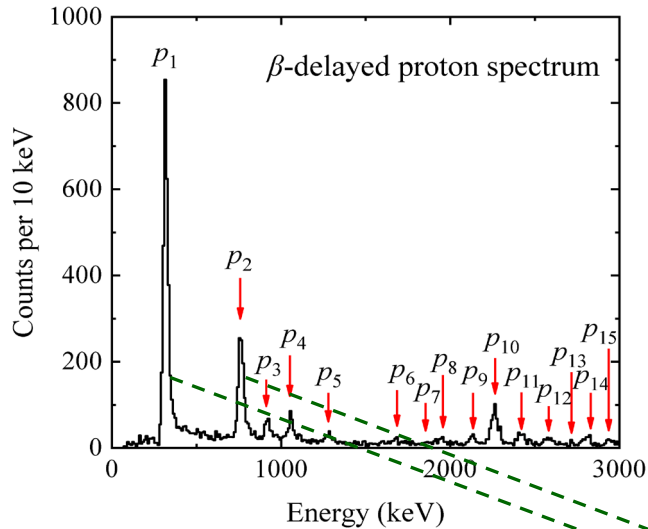
E^* (keV)	J^π	br (%)
12693(18)	$5/2^+$	

L.J. Sun *et al.*,
PRC 99, 064312 (2019).



Daughters: $^{27}\text{P}/^{26}\text{Si}$

βp & $\beta \gamma$ were measured simultaneously for the first time.



- ★ Branch ratios pinned down
- ★ Precise energy & mass data

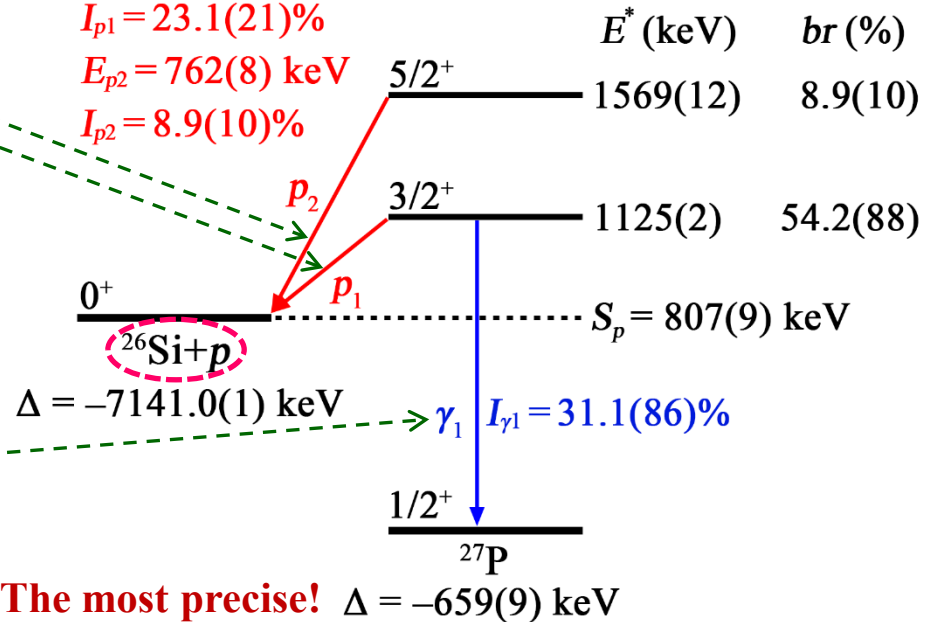
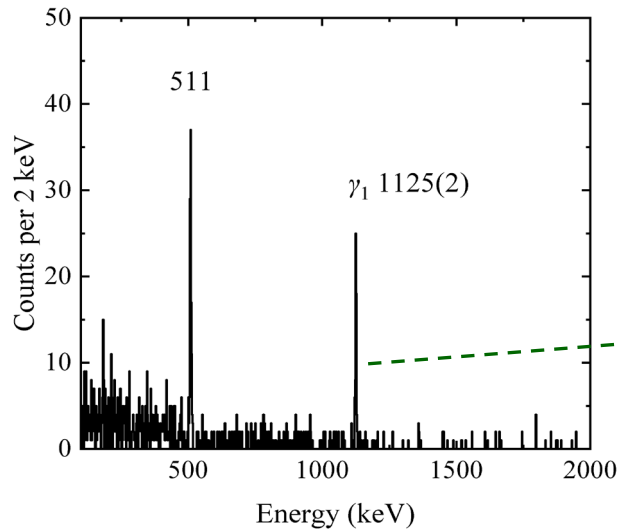
$T_{1/2} = 16.3(2)$ ms

^{27}S $5/2^+$
 $\Delta = 17638(96)$ keV

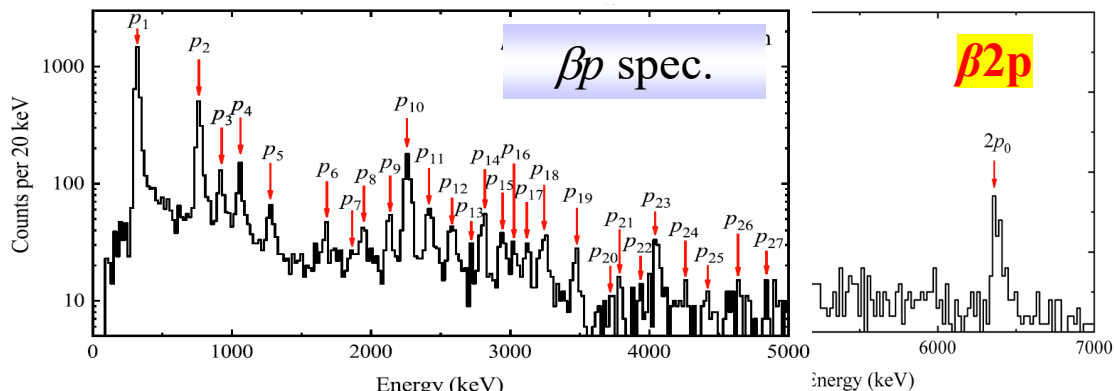
β^+

$Q_{EC} = 18297(97)$ keV

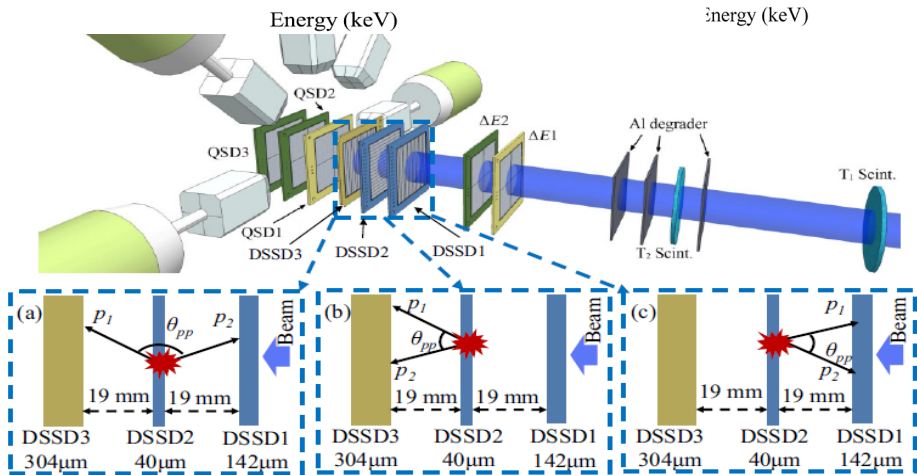
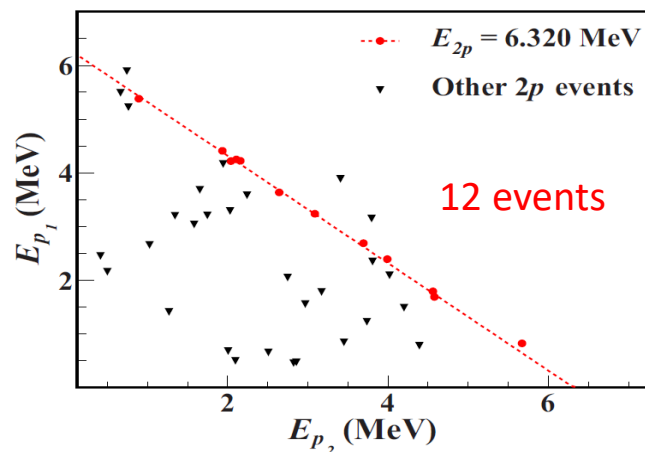
$E_{p1} = 318(8)$ keV
 $I_{p1} = 23.1(21)\%$
 $E_{p2} = 762(8)$ keV
 $I_{p2} = 8.9(10)\%$



$\beta 2p$ Decay of ^{27}S



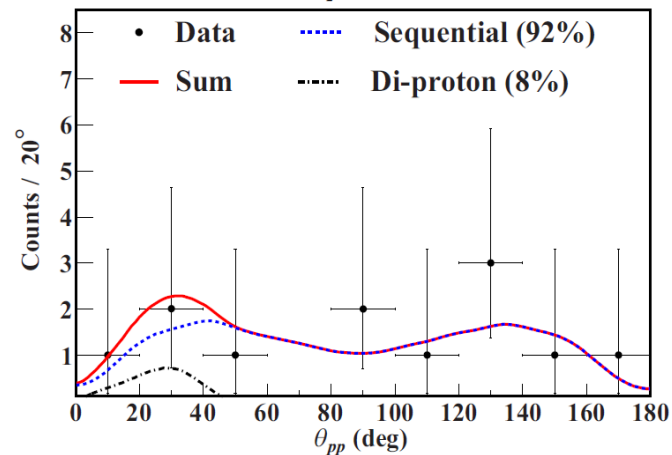
27 βp & 1 $\beta 2p$ decays



图：2p关联事件的判选

- ^{27}S β 缓发双质子发射主要是级联衰变过程。
- Referee: “such measurements are pioneering.”

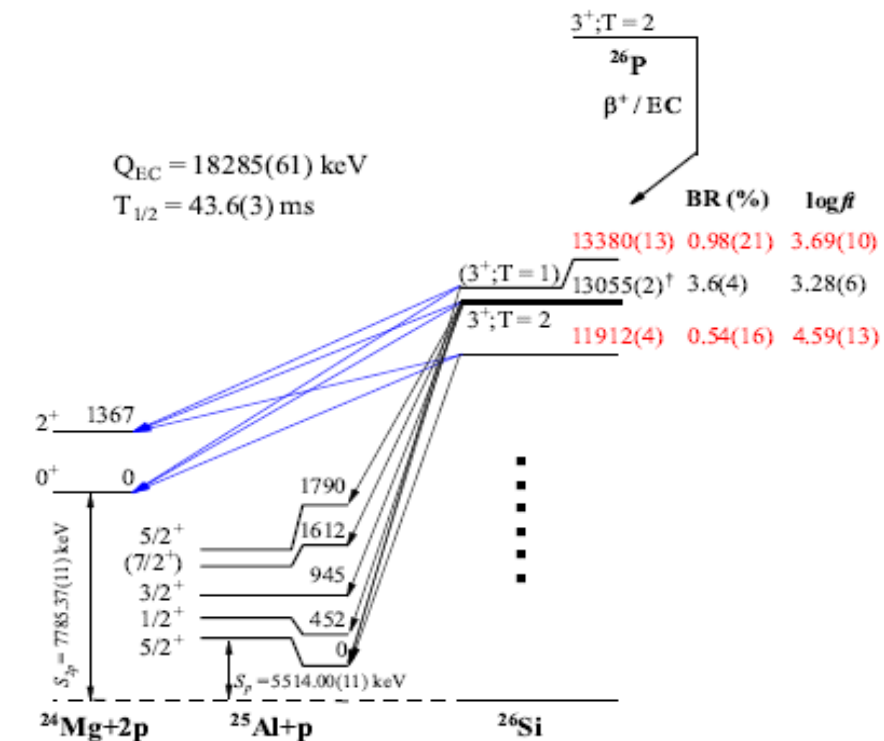
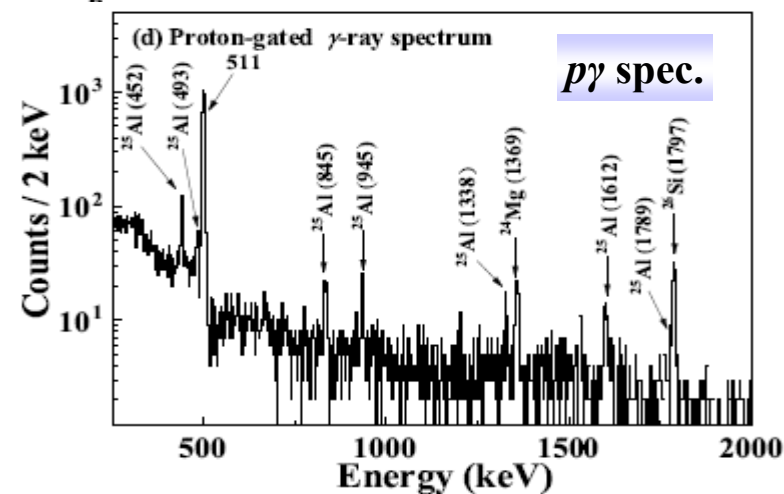
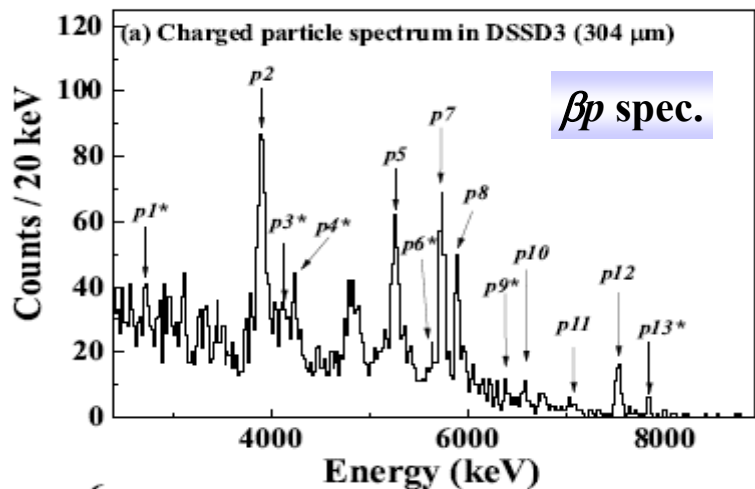
G.Z. Shi *et al.*, Phys. Rev. C **103**, L061301(2021).



^{27}S $\beta 2p$ 的能量和角关联

^{26}P Decays

★ 极强的同位旋混合态



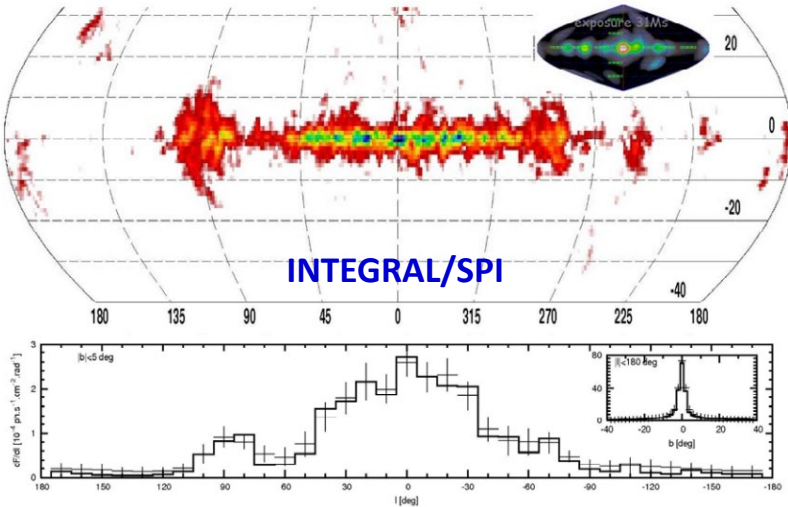
E (keV)	I_β (%)	log ft	$B(F)$	$B(GT)$
13380(13)	0.98(21)	3.69(10)	0.8(4)	0.29(13)
13055(2) ^{IAS}	3.6(4)	3.28(6)	3.2(4)	
11912(4)	0.54(16)	4.59(13)		0.099(30)

mixing angle: $\theta = 27(6)^\circ$

mixing matrix element: $\nu = 130(21) \text{ keV}$

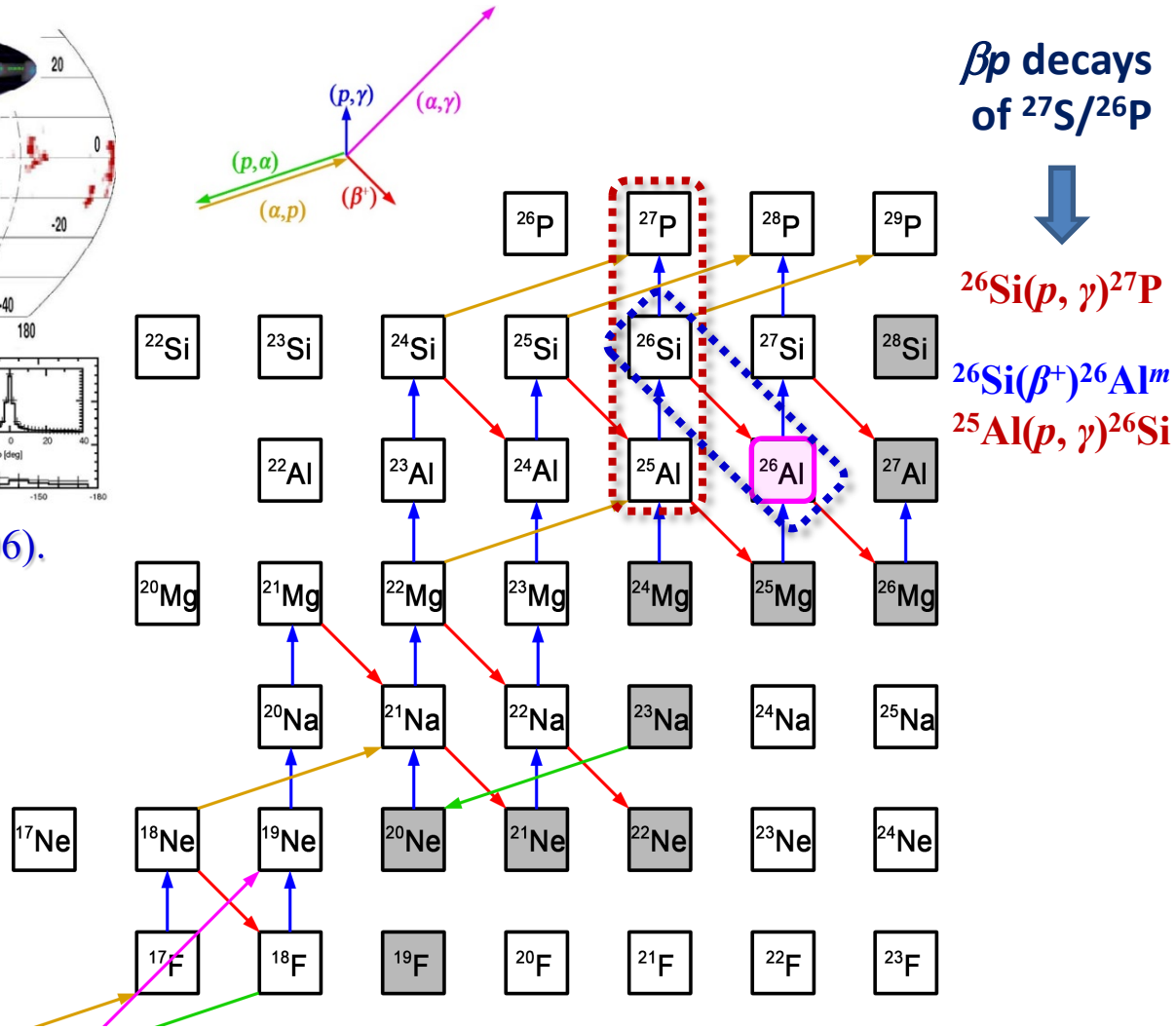
J.J. Liu *et al.*, Submitted to Phys. Rev. Lett.

The Galactic ^{26}Al Puzzle



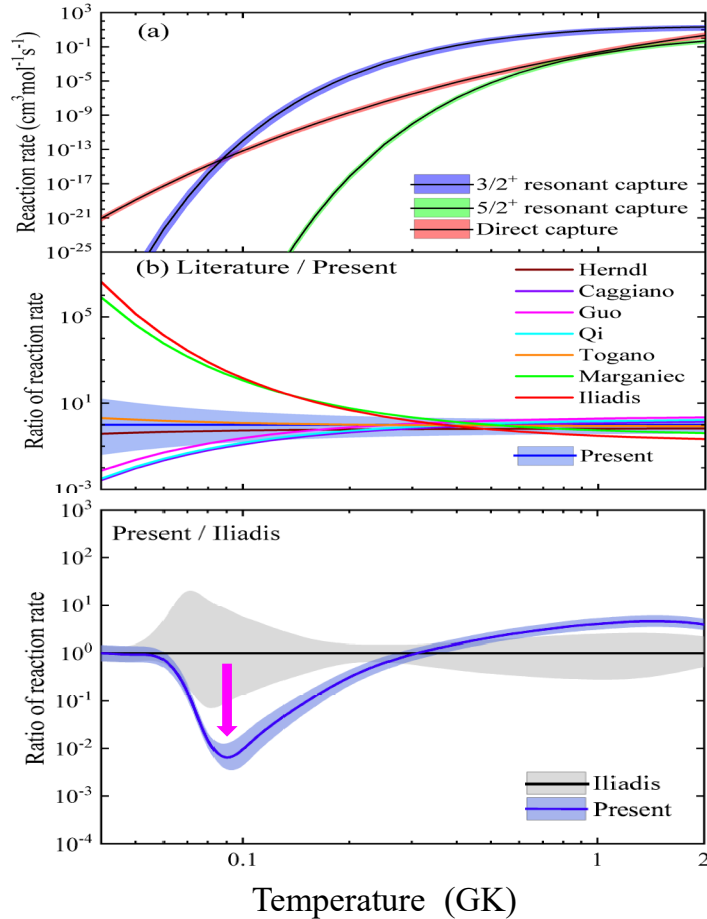
R. Diehl *et al.*, Nature **439**, 45 (2006).

The $^{26}\text{Si}(p,\gamma)^{27}\text{P}$ reaction competes with the β decay of ^{26}Si to $^{26}\text{Al}^m$, and the latter can produce $^{26}\text{Al}^g$ via thermal excitations. Thus, the production and destruction of ^{26}Si by proton capture should be influential in determining the amount of the $^{26}\text{Al}^m$ and $^{26}\text{Al}^g$ produced by the equilibrium.

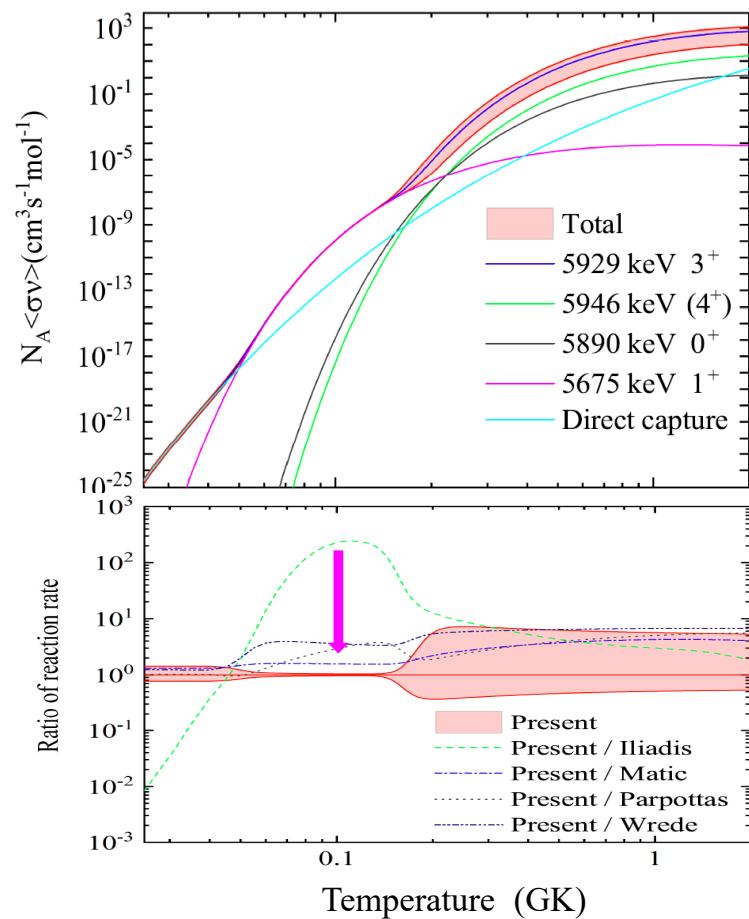


Explosive hydrogen burning scenarios

Thermonuclear Reaction Rates



L.J. Sun *et al.*,
 Phys. Lett. B **802**, 135213 (2020).



P.F. Liang *et al.*,
 Phys. Rev. C **101**, 024305 (2020).

报告内容

- 一、前言
- 二、极丰质子核的奇异衰变
- 三、奇特核的近垒反应机制
- 四、小结

奇特核反应

奇特核：弱束缚的、具有奇特结构（晕、集团）的核。奇特核反应机制研究是核物理学科一个新兴的热点方向，**破裂机制**和**连续态强耦合机制**是研究中的两个核心问题，**运动学完全测量**是关键。

♠ 弹性/准弹性散射（较多数据）

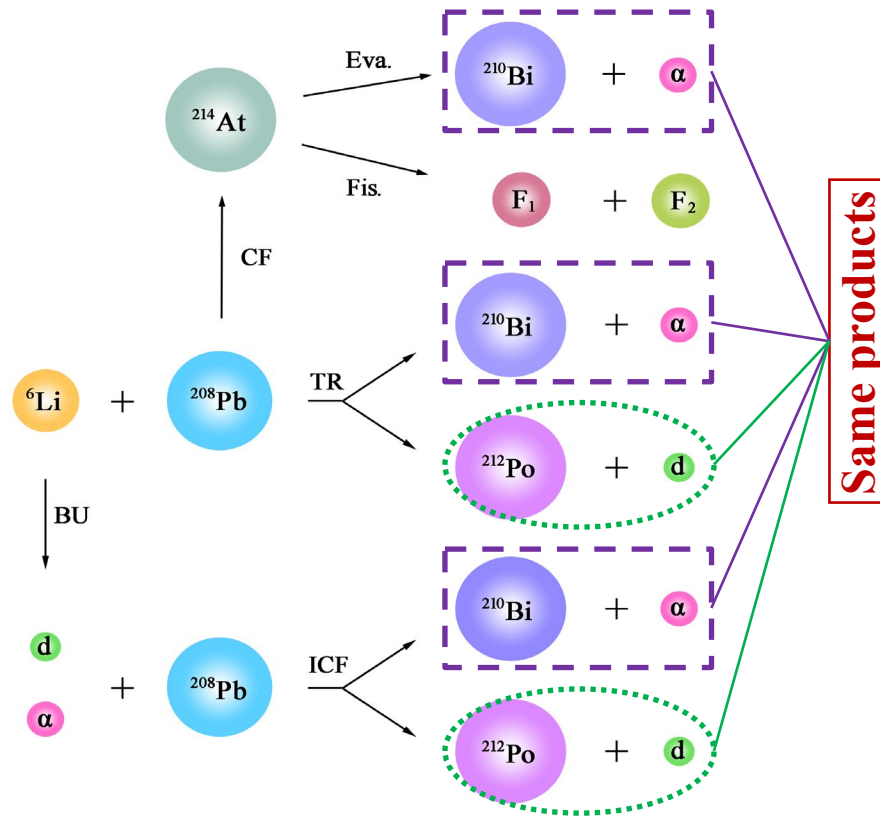
- 库仑虹抑制 ✓
- 3-body, 4-body CDCC ✓

♠ 熔合（少量数据）

- 总熔合 (TF = ICF+CF) ✓
- 不完全熔合 (ICF) ✗
- 全熔合 (CF) ✗

♠ 破裂/转移（极少数据）

- 单举测量 ✓
- 符合测量 ✗



丰质子核的反应

Reactions with light exotic nuclei ($A < 20$)

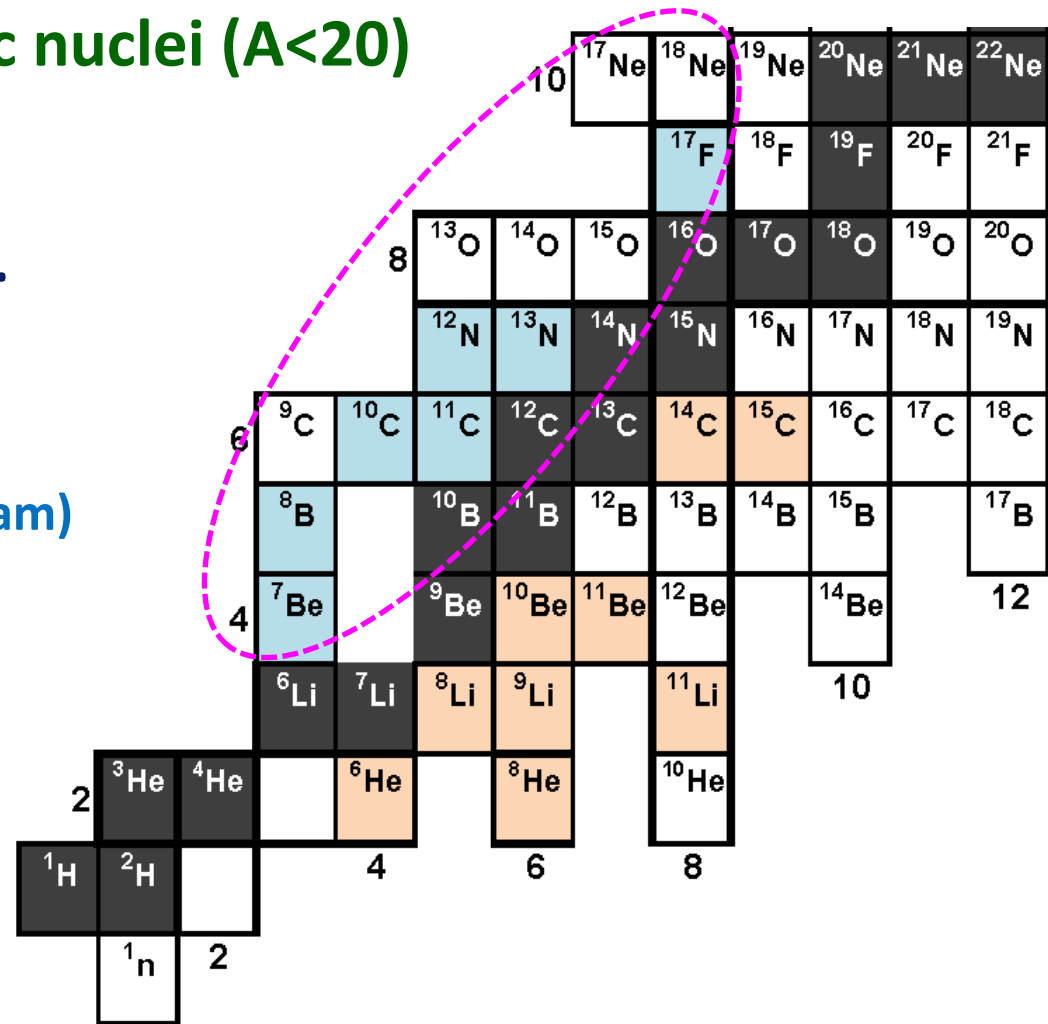
☞ Elastic, fusion, breakup ...

☞ Proton-rich nuclei

☞ ${}^7\text{Be}$, ${}^8\text{B}$, ${}^{17}\text{F}$ (Key R&D Program)

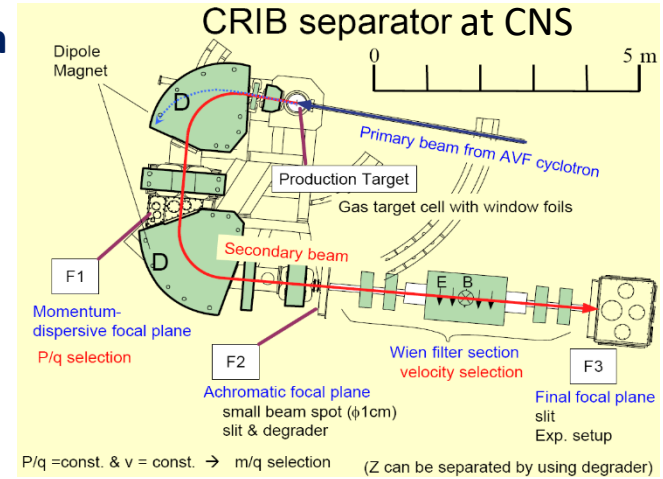
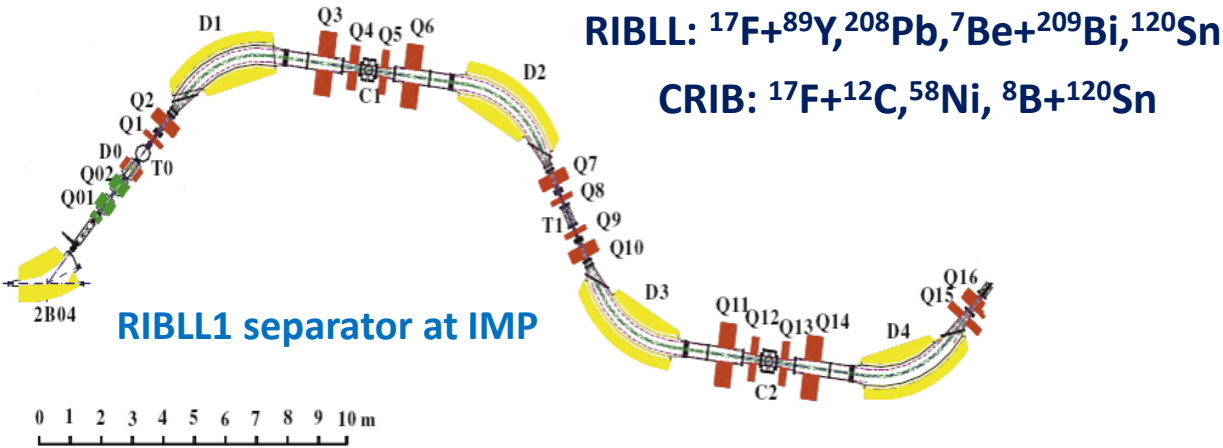
${}^{12}\text{N}$, ${}^{17,18}\text{Ne}$...

☞ **Complete-kinematics measurement**
(particle identification & large solid-angle covered)



Experiments

★ Complete-kinematics measurement ; ★ Reactions induced by ${}^7\text{Be}$, ${}^8\text{B}$, ${}^{17}\text{F}$...

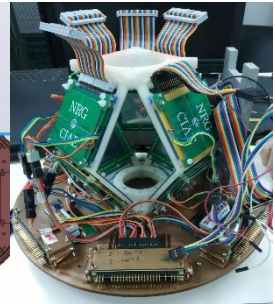
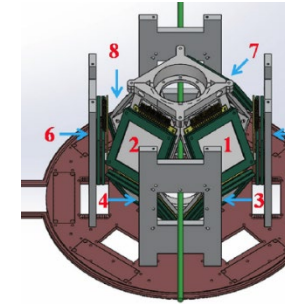
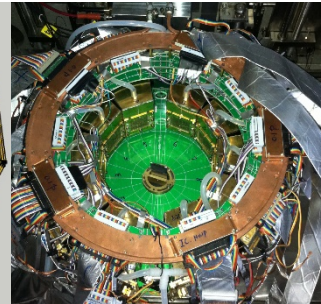
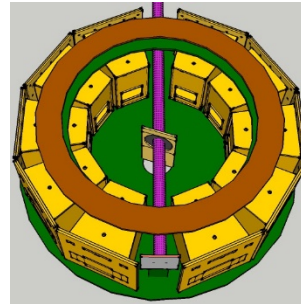
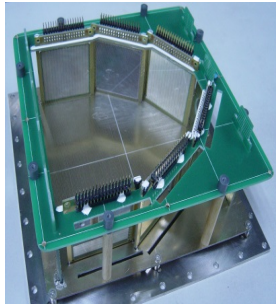


${}^{17}\text{F}+{}^{12}\text{C}$
 2007@CRIB

${}^{17}\text{F}+{}^{89}\text{Y}$
 2015@RIBLL1

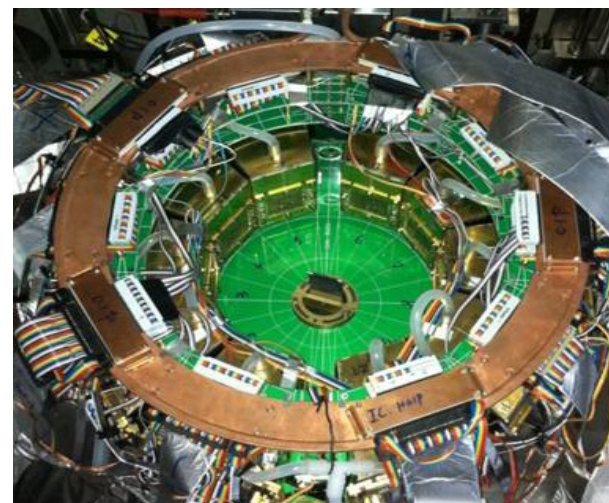
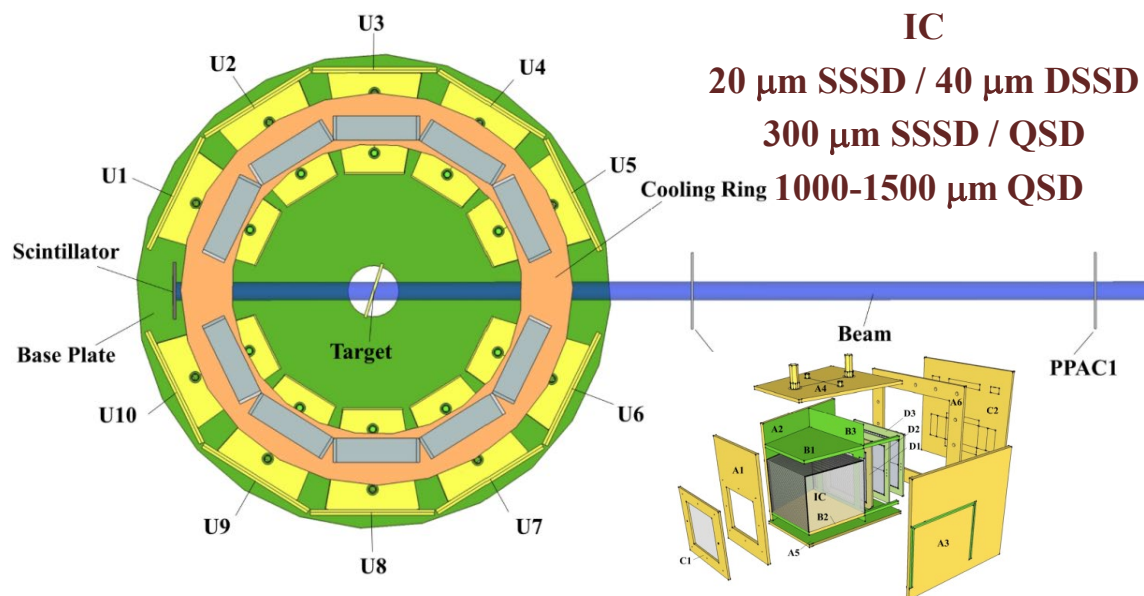
${}^{17}\text{F}+{}^{208}\text{Pb}$, 2015@RIBLL1
 ${}^{17}\text{F}+{}^{58}\text{Ni}$, 2015@CRIB

${}^7\text{Be}+{}^{209}\text{Bi}$, 2018@RIBLL1
 ${}^8\text{B}+{}^{120}\text{Sn}$, 2019@CRIB
 ${}^7\text{Be}+{}^{120}\text{Sn}$, 2021@RIBLL1



EPJA **48**, 65 (2012); PRC **97**, 044618 (2018); EPJA **57**, 143 (2021); PLB **813**, 136045 (2021) ...

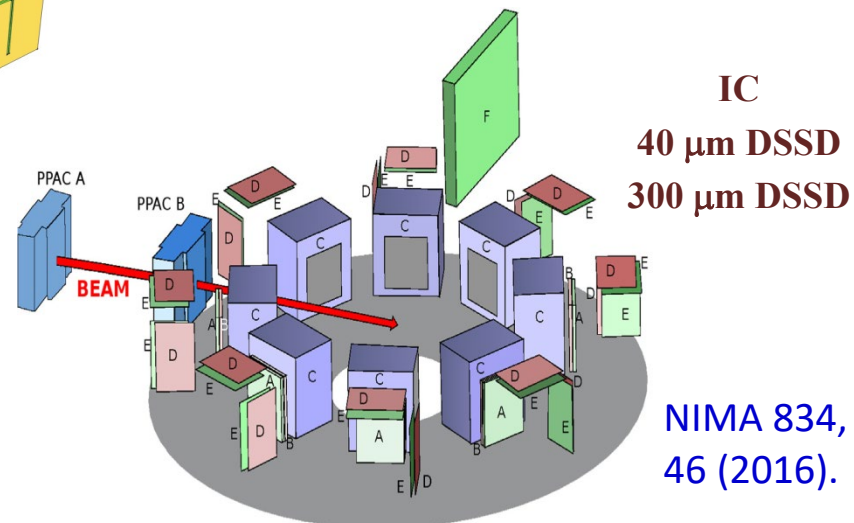
电离室多重望远镜阵列



CIAE-MITA阵列, 10组4重, 8% 4π

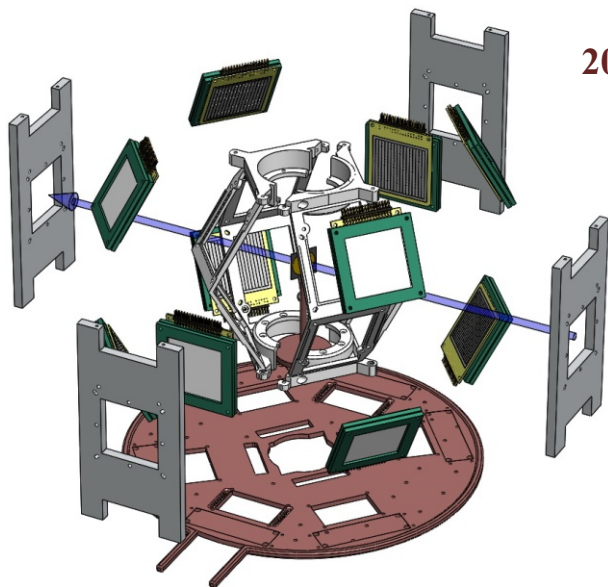
N.R. Ma et al., EPJA 55, 87 (2019). **【封面文章】**

- 运动学完全测量方法, 开展较重奇特核 (^{17}F) 的反应机制研究。
- 多层探测器组合, 兼顾轻重离子鉴别。
- PCB架构, 轻便易携带, 方便合作。



意大利EXPADES阵列, 8组3重, 5% 4π

大立体角硅条望远镜阵列

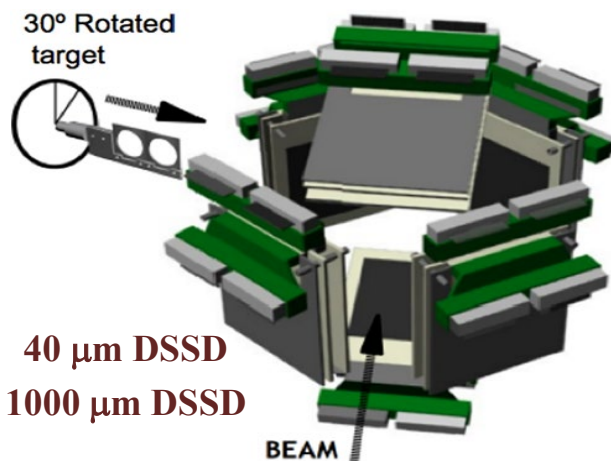
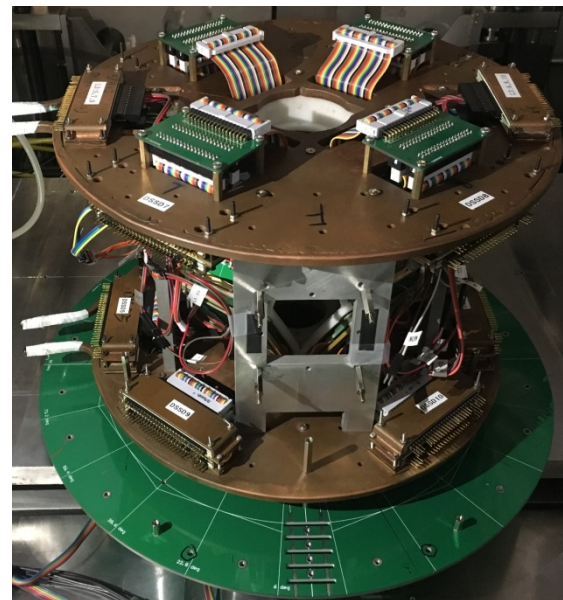


20 μm SSSD / 40 μm DSSD
300 μm SSSD / QSD
1000-1500 μm QSD

3D打印中心骨架

CIAE阵列, 10组3重, 40% 4π

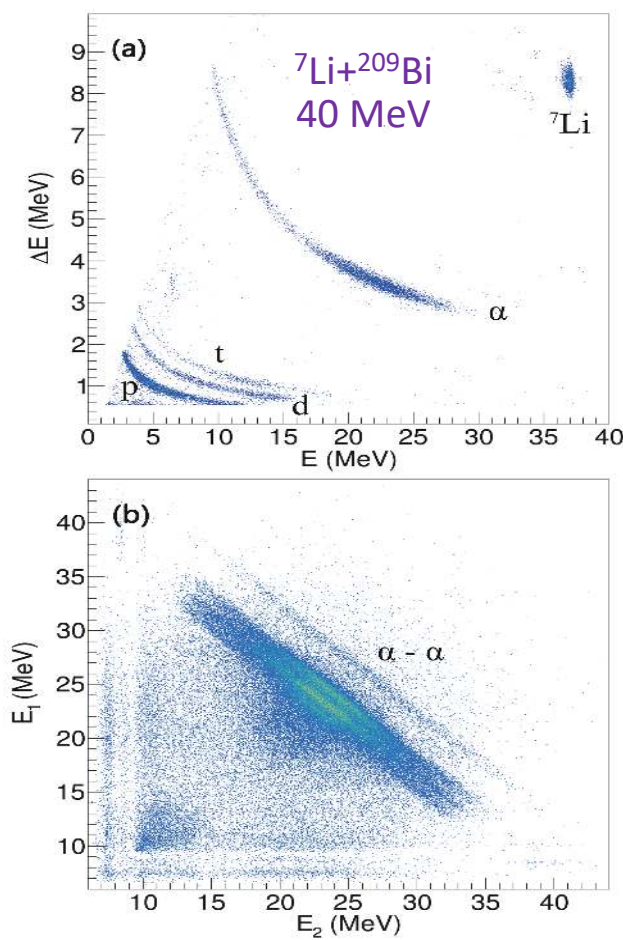
- 运动学完全测量方法, 开展较轻奇特核 (^7Be , ^8B) 的反应机制研究。
- 大立体角覆盖, $16 \times 16 \times 10 = 2560$ 点阵。
- 多层探测器组合, 离子鉴别性能优秀。



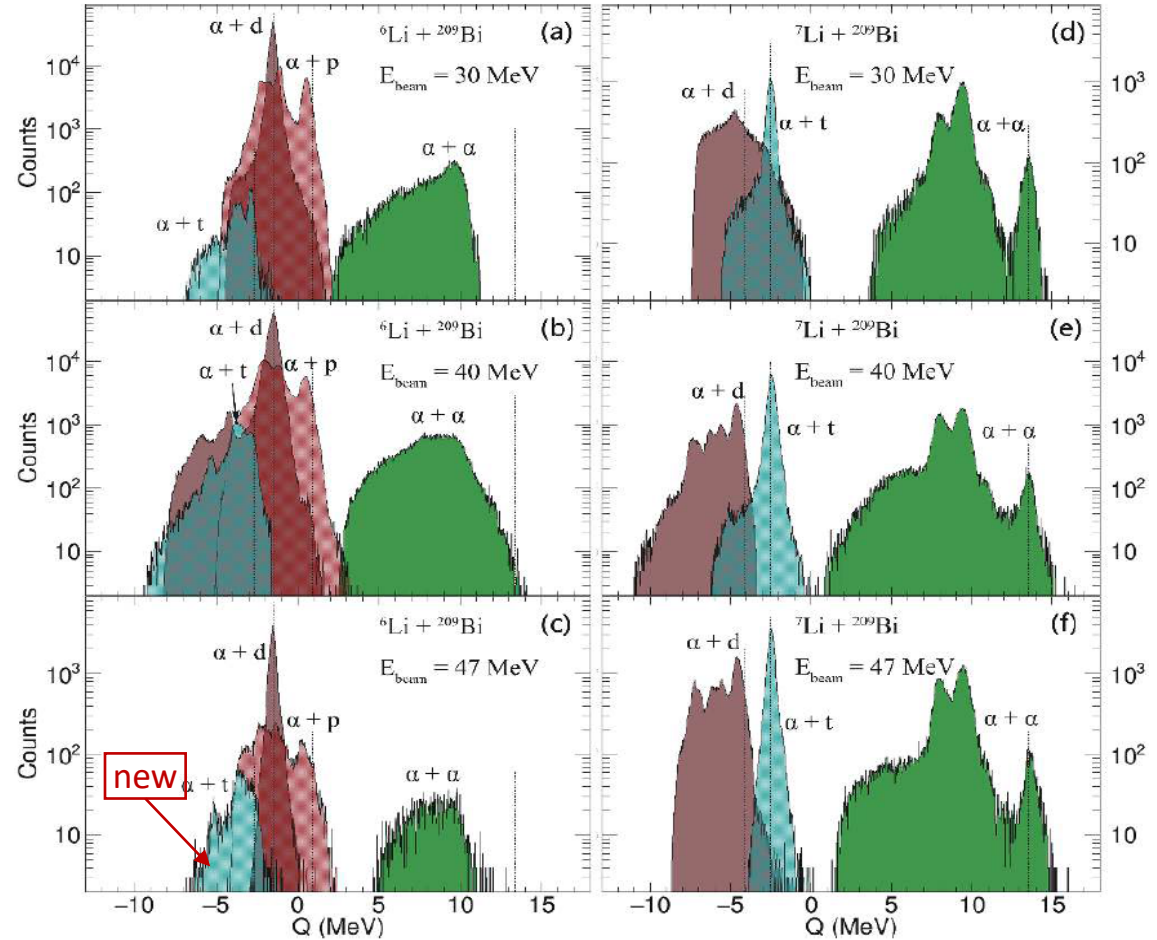
欧洲GLORIA阵列, 6组2重, 30% 4π

Results1: ${}^6,{}^7\text{Li}+{}^{209}\text{Bi}$ - 1

利用运动学完全测量详细研究了 ${}^6,{}^7\text{Li}+{}^{209}\text{Bi}$ 在30, 40, and 47 MeV的反应机制。



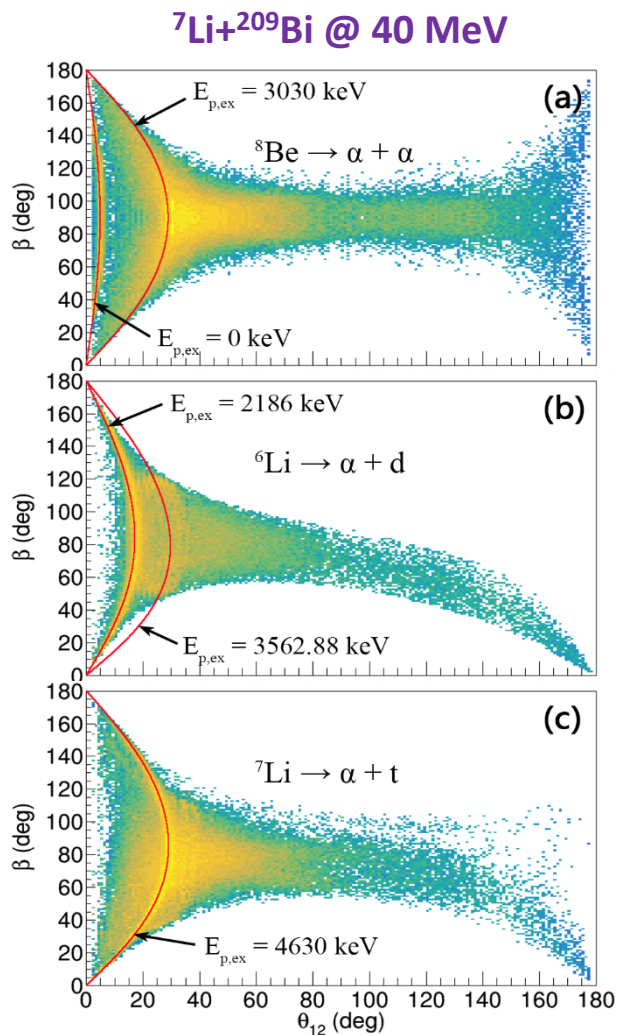
探测器粒子鉴别图和关联图



不同破裂道Q值谱

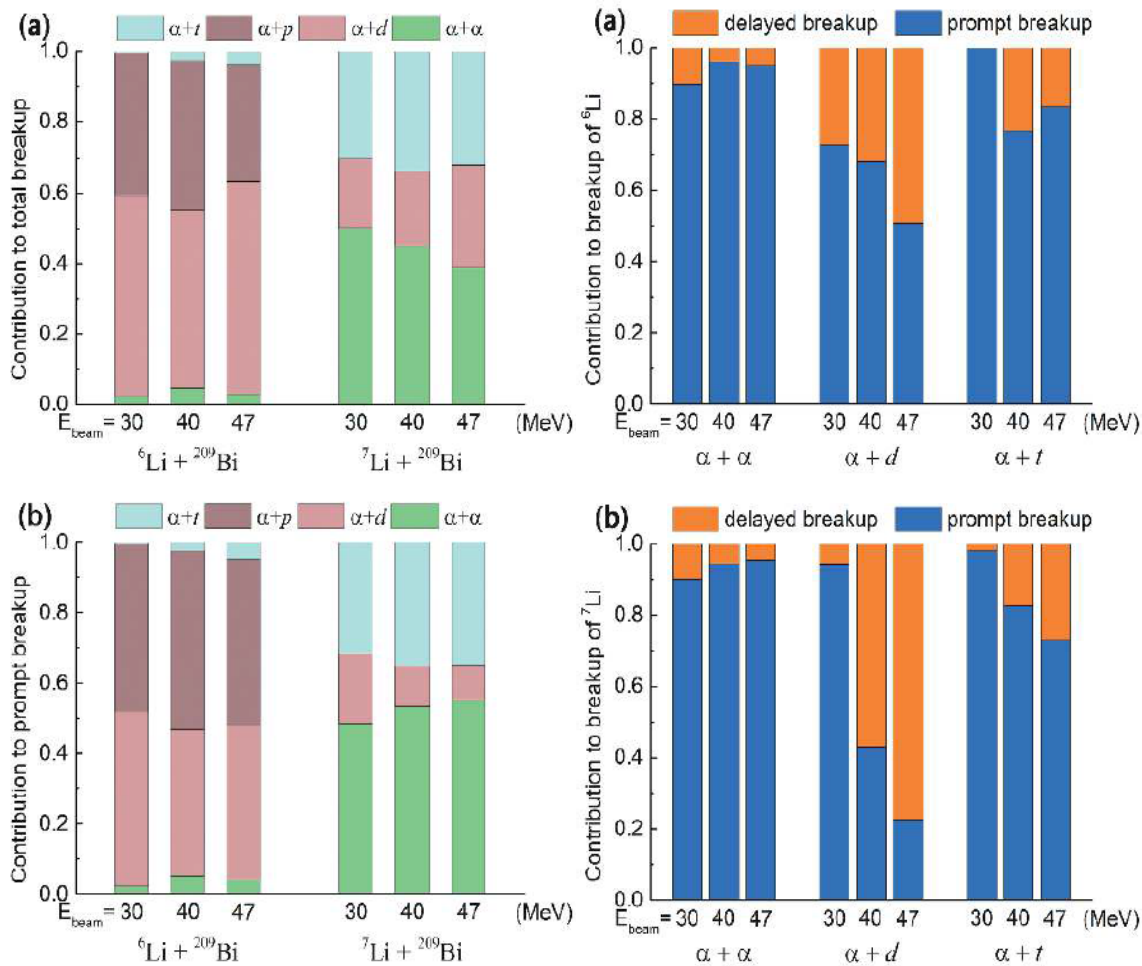
Y.J. Yao *et al.*, Nucl. Sci. Tech. 32, 14 (2021); Chin. Phys. C 45, 054104 (2021).

Results1: ${}^6,{}^7\text{Li}+{}^{209}\text{Bi}$ - 2



破裂子体角关联

${}^6,{}^7\text{Li}+{}^{209}\text{Bi}$ @ 30,40,47 MeV

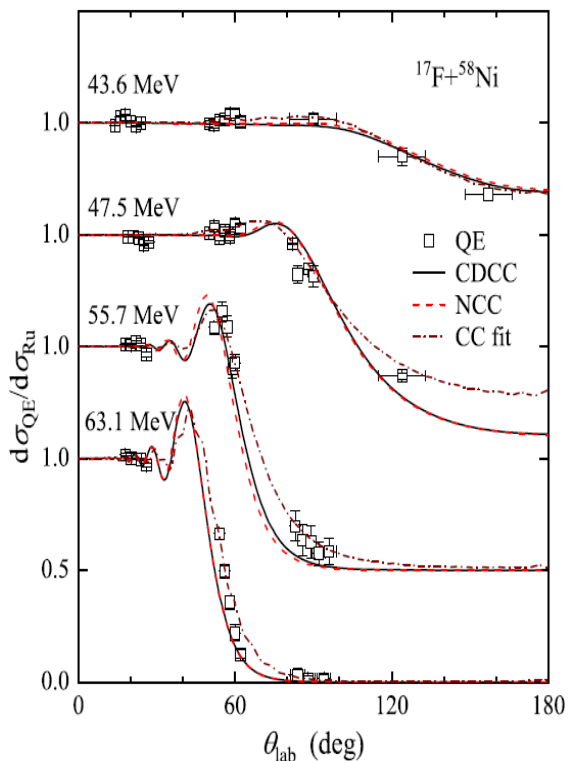


不同破裂道、不同破裂时标的分支比

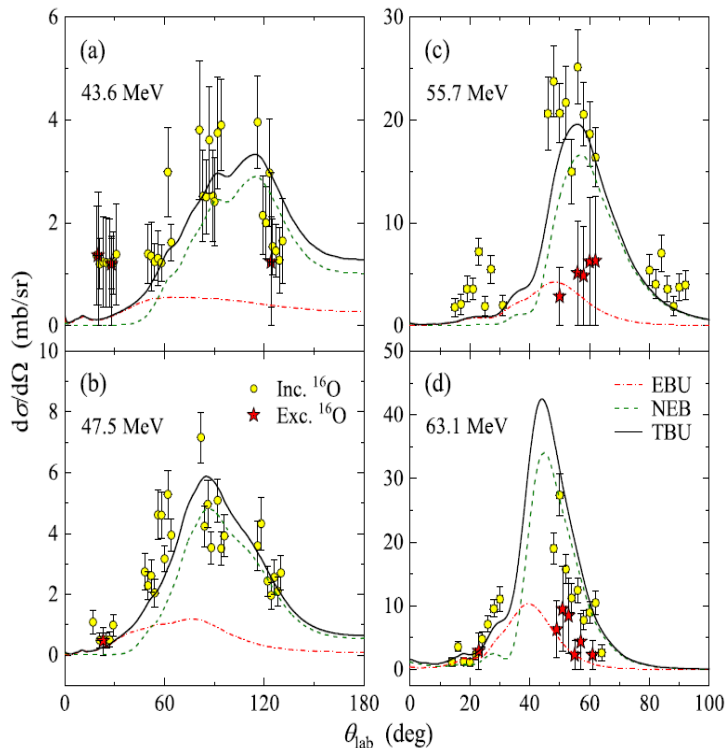
Y.J. Yao *et al.*, Nucl. Sci. Tech. 32, 14 (2021); Chin. Phys. C 45, 054104 (2021).

Results2: $^{17}\text{F}+^{58}\text{Ni}$

★ 运动学完全测量，首次在近垒能区获得带电粒子的全反应道的数据。



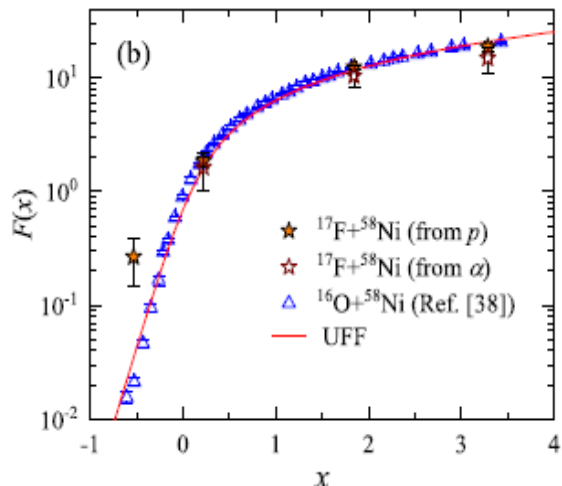
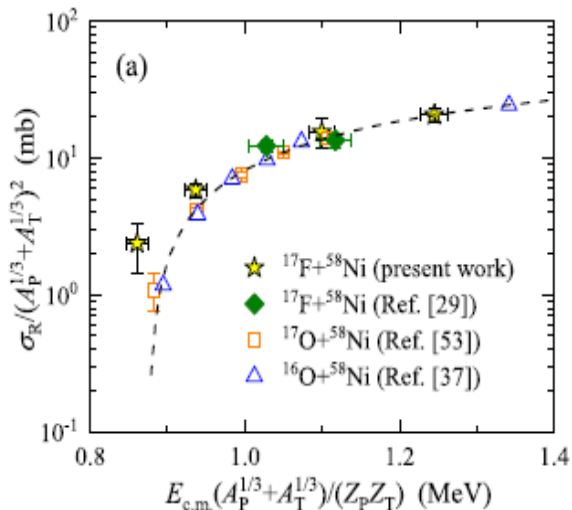
准弹性散射角分布



破裂/转移角分布

- 采用CC、CDCC、IAV、PLATYPUS等模型分析；
- 非弹性破裂为主；垒下反应截面和全融合截面增强。

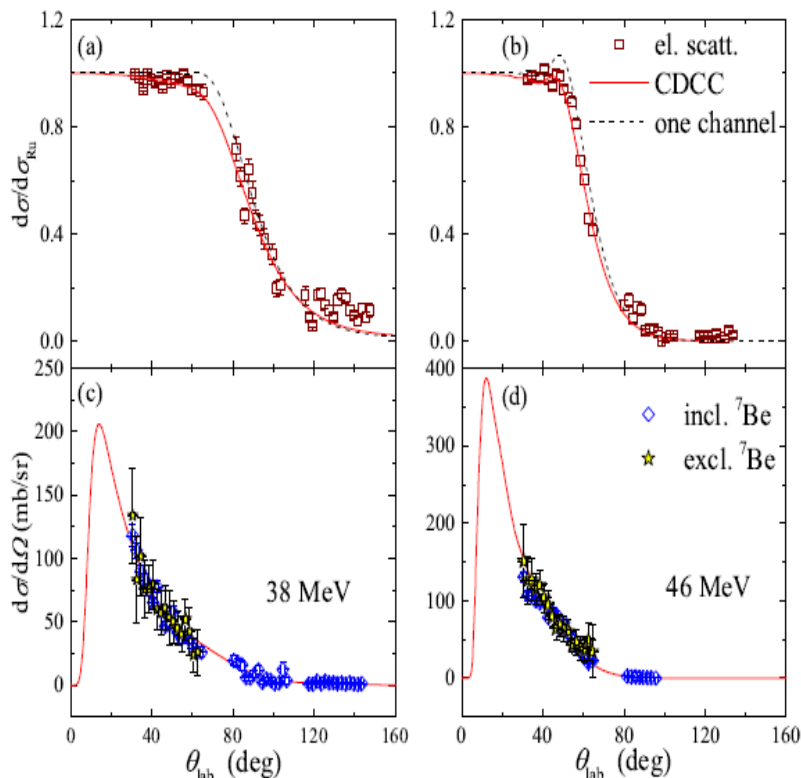
L. Yang *et al.*, Phys. Lett. B 813, 136045 (2021).



反应(上)和全融合(下)激发函数

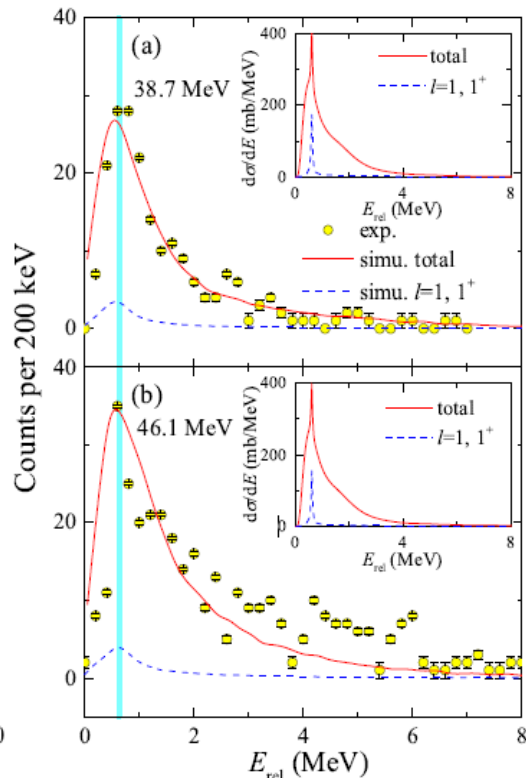
Results3: $^8\text{B}+^{120}\text{Sn}$

★ 运动学完全测量，首次在近垒能区获得 ^8B 破裂子体($^7\text{Be}+p$)的关联数据。



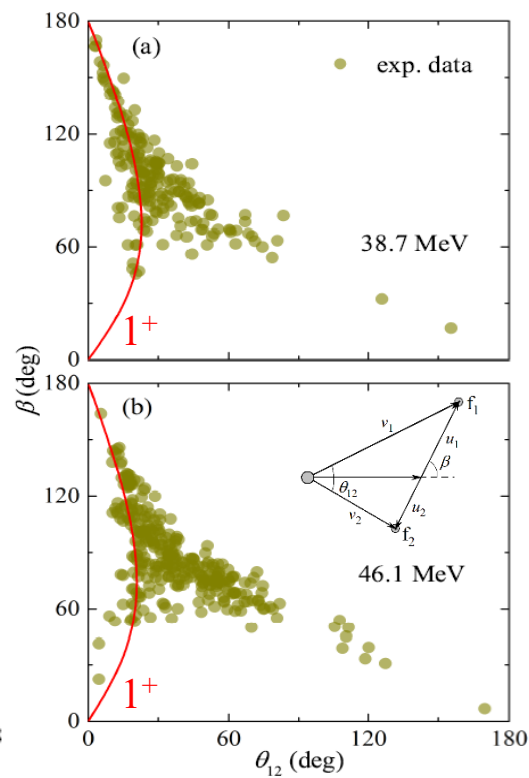
准弹、Inc和Exc破裂角分布

- Exc破裂截面几乎等于Inc破裂截面，弹性破裂为主；



^7Be -p相对能量分布

- CDCC计算， 1^+ 共振态贡献仅占4%；

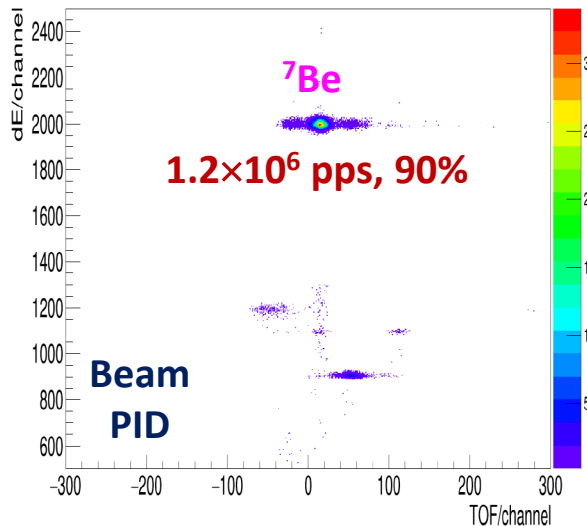


^7Be -p角关联

- 出射道瞬时破裂破裂为主。

L. Yang *et al.*, submitted to Nature Communications.

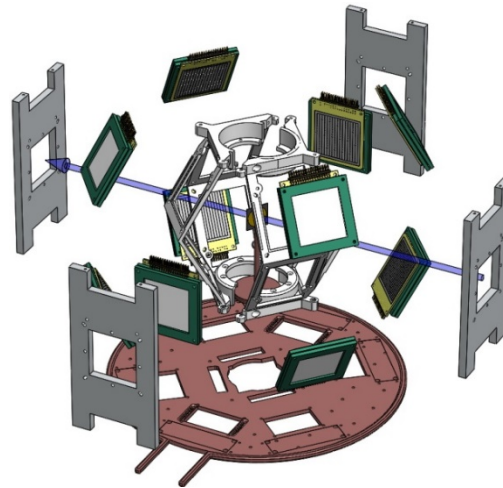
In Progress: ${}^7\text{Be}+{}^{209}\text{Bi}, {}^{120}\text{Sn}$



$p({}^7\text{Li}, {}^7\text{Be})n$

${}^7\text{Li}$: 8.8 MeV/u, 1.5 euA

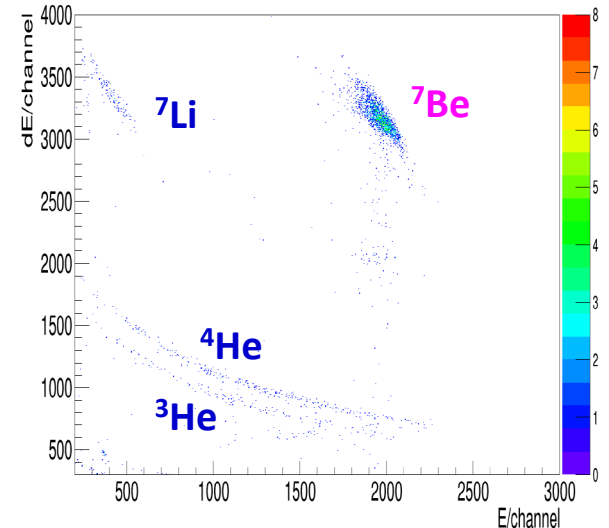
H_2 gas: 1000 mbar, 8 cm, 90 K



20/40 μm SSD + 300 μm QSD + 1.5mm QSD

10 group of $\Delta\text{E}-\Delta\text{E}-\text{E}$ telescopes

40% of 4π



$\Delta\text{E}-\Delta\text{E}$ spectrum

by 40 μm DSSD & 300 μm QSD
(1 strip, 1 run, 2 hours)

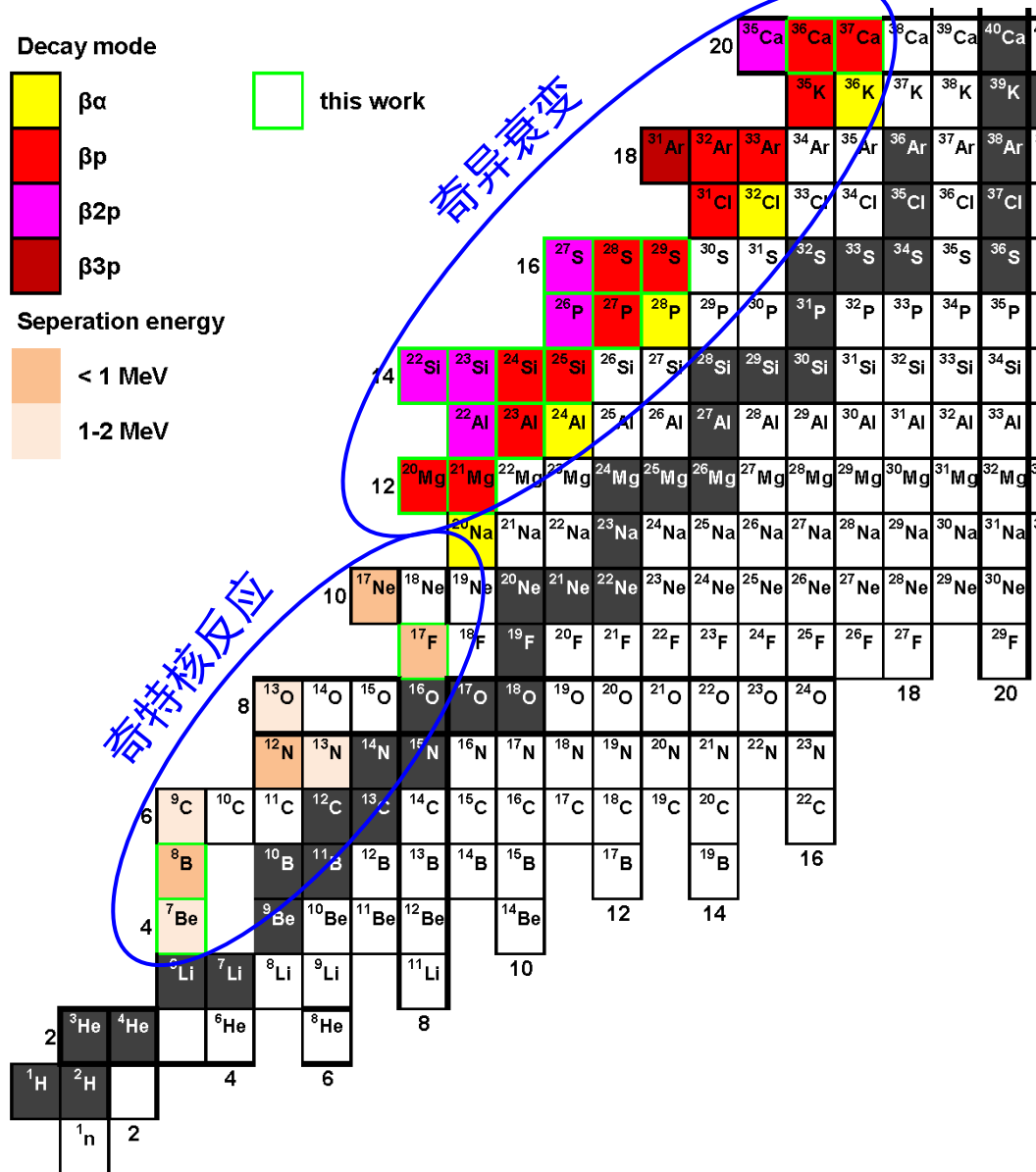
1. Exclusive breakup: ${}^7\text{Be} \rightarrow {}^3\text{He}+{}^4\text{He}$ (coin. Eff. $\sim 10\%$ by MC simulations);
2. ${}^4\text{He}$ stripping: ${}^7\text{Be}+{}^{209}\text{Bi} \rightarrow {}^3\text{He}+{}^{213}\text{At}$;
3. ${}^3\text{He}$ stripping: ${}^7\text{Be}+{}^{209}\text{Bi} \rightarrow {}^4\text{He}+{}^{212}\text{At}$;
4. $1n$ stripping: ${}^7\text{Be}+{}^{209}\text{Bi} \rightarrow {}^6\text{Be}(\rightarrow {}^4\text{He}+p+p)+{}^{210}\text{Bi}$;
5. $1n$ pickup: ${}^7\text{Be}+{}^{209}\text{Bi} \rightarrow {}^8\text{Be}(\rightarrow {}^4\text{He}+{}^4\text{He})+{}^{208}\text{Bi}$;
6. $1p$ stripping: ${}^7\text{Be}+{}^{209}\text{Bi} \rightarrow {}^6\text{Li}(\rightarrow {}^4\text{He}+d)+{}^{210}\text{Po}$;
7. $1p$ pickup: ${}^7\text{Be}+{}^{209}\text{Bi} \rightarrow {}^8\text{B}(\rightarrow ???)+{}^{208}\text{Pb}$;
9. Fusion: ${}^7\text{Be}+{}^{209}\text{Bi} \rightarrow {}^{216}\text{Fr} \rightarrow \alpha, p, n$ eva. & decay (energy & angular distri.)

ICF (Ene-Ang corr.)

小结

1) **奇异衰变**: 高精度测量了sd壳层15个丰质子核的 β 延迟衰变, 获得了丰富的谱学信息, 深入理解了核结构性质及其有效相互作用。

2) **奇特核反应**: 运动学完全测量了 ${}^7\text{Be}$ 、 ${}^8\text{B}$ 和 ${}^{17}\text{F}$ 与不同靶核的反应, 获得了带电粒子全反应道的信息, 深入理解了破裂机制及其连续态耦合机制。



Thanks to all the collaborators!

for example

PHYSICAL REVIEW C 99, 064312 (2019)

Physics Letters B 813 (2021) 136045

β -decay spectroscopy of ^{27}S

L. J. Sun (孙立杰),^{1,2,3} X. X. Xu (徐新星),^{1,2,4} C. J. Lin (林承键),^{1,4,†} J. Lee (李晓菁),^{2,‡} S. Q. Hou (侯素青),⁵
C. X. Yuan (袁岑溪),⁶ Z. H. Li (李智焕),⁷ J. José,^{8,9,§} J. J. He (何建军),^{10,11} J. S. Wang (王建松),⁵ D. X. Wang (王东玺),¹
H. Y. Wu (吴鸿毅),⁷ P. F. Liang (梁鹏飞),² Y. Y. Yang (杨彦云),⁵ Y. H. Lam (蓝乙华),⁵ P. Ma (马朋),⁵
F. F. Duan (段芳芳),^{12,5} Z. H. Gao (高志浩),^{5,12} Q. Hu (胡强),⁵ Z. Bai (白真),⁵ J. B. Ma (马军兵),⁵ J. G. Wang (王建国),⁵
F. P. Zhong (钟福鹏),^{4,1} C. G. Wu (武晨光),⁷ D. W. Luo (罗迪雯),⁷ Y. Jiang (蒋颖),⁷ Y. Liu (刘洋),⁷ D. S. Hou (侯东升),^{5,11}
R. Li (李忍),^{5,11} N. R. Ma (马南茹),¹ W. H. Ma (马维虎),^{5,13} G. Z. Shi (石国柱),⁵ G. M. Yu (余功明),⁵ D. Patel,⁵
S. Y. Jin (金树亚),^{5,11} Y. F. Wang (王煜峰),^{14,5} Y. C. Yu (余悦超),^{14,5} Q. W. Zhou (周清武),^{15,5} P. Wang (王鹏),^{15,5}
L. Y. Hu (胡力元),¹⁶ X. Wang (王翔),⁷ H. L. Zang (臧宏亮),⁷ P. J. Li (李朋杰),² Q. Q. Zhao (赵青青),² L. Yang (杨磊),¹
P. W. Wen (温培威),¹ F. Yang (杨峰),¹ H. M. Jia (贾会明),¹ G. L. Zhang (张高龙),¹⁷ M. Pan (潘敏),^{17,1}
X. Y. Wang (汪小雨),¹⁷ H. H. Sun (孙浩瀚),¹ Z. G. Hu (胡正国),⁵ R. F. Chen (陈若富),⁵ M. L. Liu (柳敏良),⁵
W. Q. Yang (杨维青),⁵ Y. M. Zhao (赵玉民),³ and H. Q. Zhang (张焕乔)¹

(RIBLL Collaboration)

¹Department of Nuclear Physics, China Institute of Atomic Energy, Beijing 102413, China

²Department of Physics, The University of Hong Kong, Hong Kong, China

³School of Physics and Astronomy, Shanghai Jiao Tong University, Shanghai 200240, China

⁴College of Physics and Technology, Guangxi Normal University, Guilin 541004, China

⁵Institute of Modern Physics, Chinese Academy of Sciences, Lanzhou 730000, China

⁶Sino-French Institute of Nuclear Engineering and Technology, Sun Yat-Sen University, Zhuhai 519082, China

⁷State Key Laboratory of Nuclear Physics and Technology, School of Physics, Peking University, Beijing 100871, China

⁸Departament de Física, Escola d'Enginyeria de Barcelona Est, Universitat Politècnica de Catalunya, Av. J. Eduard Maristany 10, E-08930 Barcelona, Spain

⁹Institut d'Estudis Espacials de Catalunya, Ed. Nexus-201, C/ Gran Capità 2-4, E-08034 Barcelona, Spain

¹⁰College of Nuclear Science and Technology, Beijing Normal University, Beijing 100875, China

¹¹University of Chinese Academy of Sciences, Beijing 100049, China

¹²School of Nuclear Science and Technology, Lanzhou University, Lanzhou 730000, China

¹³Institute of Modern Physics, Fudan University, Shanghai 200433, China

¹⁴School of Physics and Astronomy, Yunnan University, Kunming 650091, China

¹⁵School of Physical Science and Technology, Southwest University, Chongqing 400044, China

¹⁶Fundamental Science on Nuclear Safety and Simulation Technology Laboratory, Harbin Engineering University, Harbin 150001, China

¹⁷School of Physics and Nuclear Energy Engineering, Beihang University, Beijing 100191, China



ELSEVIER

Contents lists available at ScienceDirect

Physics Letters B

www.elsevier.com/locate/physletb



Insight into the reaction dynamics of proton drip-line nuclear system $^{17}\text{F}+^{58}\text{Ni}$ at near-barrier energies

L. Yang^a, C.J. Lin^{a,p,*}, H. Yamaguchi^{b,c}, Jin Lei^{d,1}, P.W. Wen^a, M. Mazzocco^{e,f}, N.R. Ma^a,
L.J. Sun^{a,2}, D.X. Wang^a, G.X. Zhang^{g,3}, K. Abe^b, S.M. Cha^h, K.Y. Chae^h, A. Diaz-Torresⁱ,
J.L. Ferreira^j, S. Hayakawa^b, H.M. Jia^a, D. Kahl^{b,4}, A. Kim^k, M.S. Kwag^h, M. La Commara^l,
R. Navarro Pérez^m, C. Parascandoloⁿ, D. Pierroutsakouⁿ, J. Rangel^j, Y. Sakaguchi^b,
C. Signorini^{e,f}, E. Strano^{e,f}, X.X. Xu^a, F. Yang^a, Y.Y. Yang^o, G.L. Zhang^g, F.P. Zhong^{a,p},
J. Lubian¹

^aChina Institute of Atomic Energy, P. O. Box 275(10), Beijing 102413, China

^bCenter for Nuclear Study, University of Tokyo, RIKEN campus, 2-1 Hirosawa, Wako, Saitama 351-0198, Japan

^cNational Astronomical Observatory of Japan, 2-21-1 Osawa, Mitaka, Tokyo 181-8588, Japan

^dInstitute of Nuclear and Particle Physics, and Department of Physics and Astronomy, Ohio University, Athens, OH 45701, USA

^eDipartimento di Fisica e Astronomia, Università di Padova, via F. Marzolo 8, I-35131 Padova, Italy

^fIstituto Nazionale di Fisica Nucleare-Sezione di Padova, via F. Marzolo 8, I-35131 Padova, Italy

^gSchool of Physics, Beihang University, Beijing 100191, China

^hDepartment of Physics, Sungkyunkwan University, Suwon 16419, Republic of Korea

ⁱDepartment of Physics, University of Surrey, Guildford GU2 7XH, United Kingdom

^jInstituto de Física, Universidade Federal Fluminense, Avenida Litorânea s/n, Gragoatá, Niterói, Rio de Janeiro 24210-340, Brazil

^kDepartment of Science Education, Ewha Womans University, Seoul 02760, Republic of Korea

^lDepartment of Pharmacy, Università Federico II, via D. Montesano 49, I-80131 Napoli, Italy

^mDepartment of Physics, San Diego State University, 5500 Campanile Drive, San Diego, CA 02182-1233, USA

ⁿIstituto Nazionale di Fisica Nucleare-Sezione di Napoli, Via Cintia, I-80126 Napoli, Italy

^oInstitute of Modern Physics, Chinese Academy of Sciences, Lanzhou 730000, China

^pDepartment of Physics, Guangxi Normal University, Guilin 541004, China



谢谢关注!



Appendix:

Optical Potential of Exotic Nuclear System

Optical Model Potential

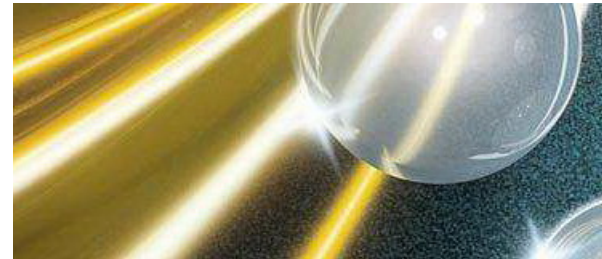
- ♠ Optical Model is a successful model to explain the nuclear scattering and reaction, which resembles the case of light scattered by an opaque glass sphere.

Optical Model Potential (OMP):

$$U = V(r) + iW(r)$$

↙
attractive

↘
absorptive



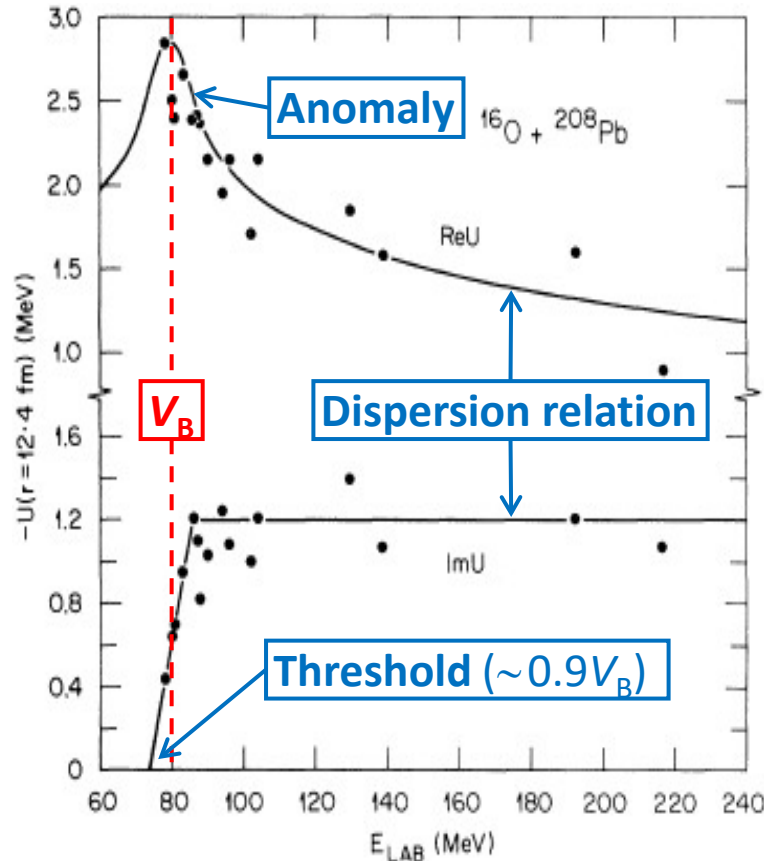
- ★ phenomenological potential, independent on energy.
- ♠ A basic task in nuclear reaction study is to understand the nucleus-nucleus interaction.

Cf: 1) S. Fernbach, R. Serber, and T. B. Taylor, Phys. Rev. **73**, 1352 (1949).

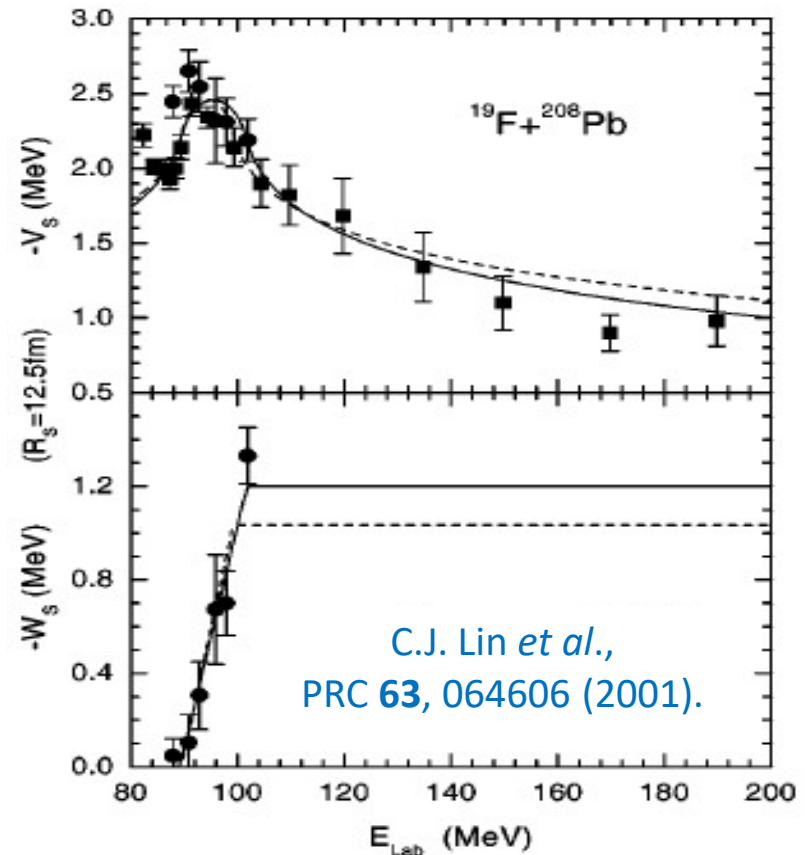
2) H. Feshbach, "The optical model and its justification", Ann. Rev. Nucl. Sci. **8**, 49 (1958).

Tightly-bound-nuclei Systems

Threshold Anomaly



A universal phenomenon within the Coulomb barrier energy region

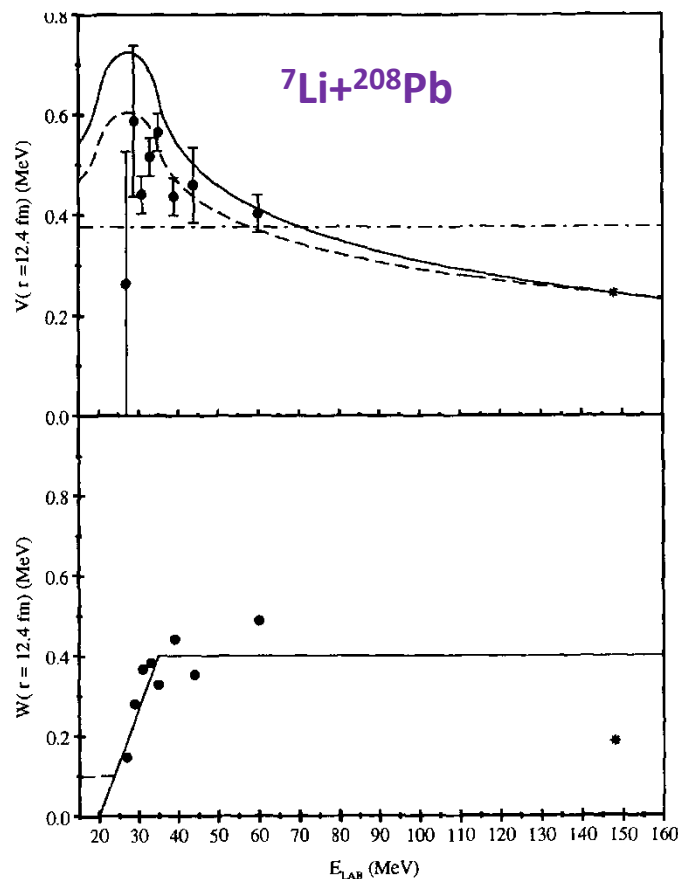


C.J. Lin *et al.*,
PRC **63**, 064606 (2001).

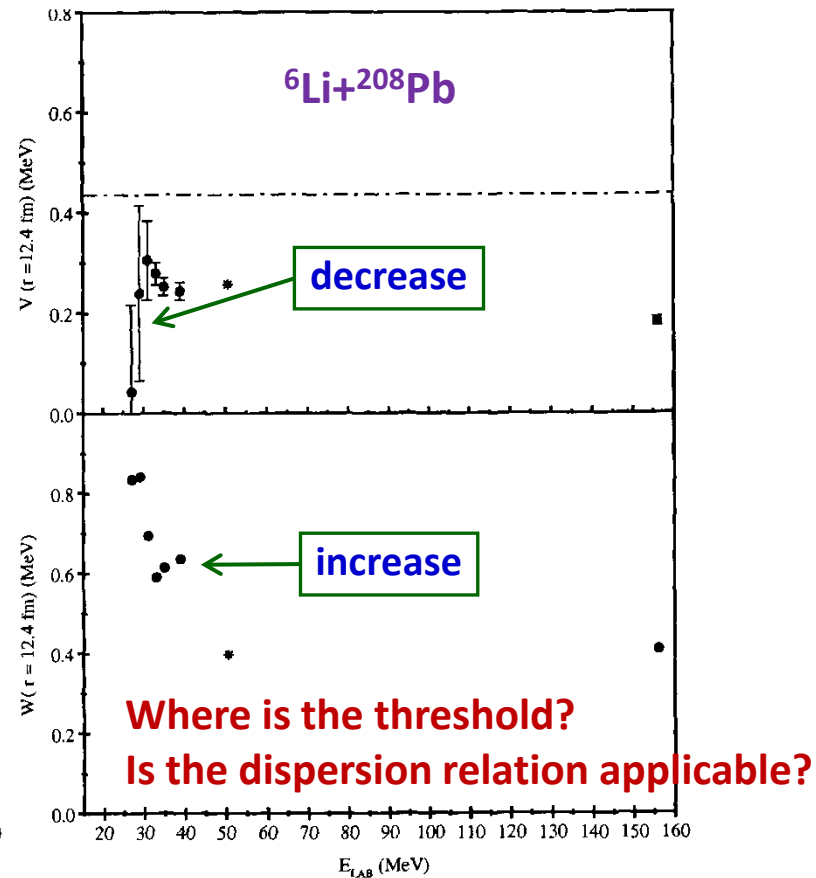
- Cf: 1) M. A. Nagarajan, C. C. Mahaux, and G. R. Satchler, Phys. Rev. Lett. **54**, 1136 (1985).
 2) C. Mahaux, H. Ngo, and G. R. Satchler, Nucl. Phys. **A449**, 354 (1986).
 3) G. R. Satchler, Phys. Rep. **199**, 147 (1991).

Weakly-bound-nuclei Systems

Threshold Anomaly



Abnormal Threshold Anomaly

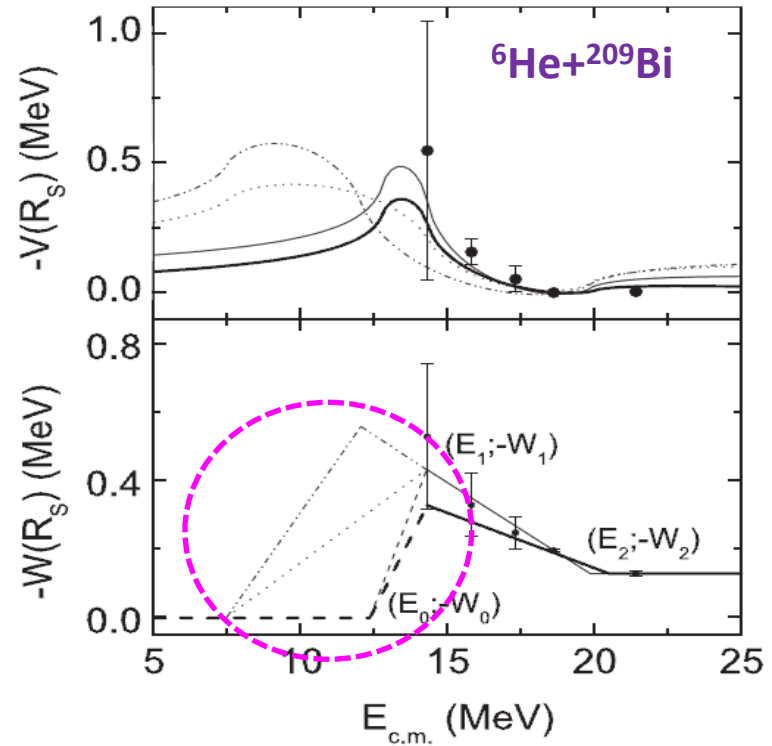
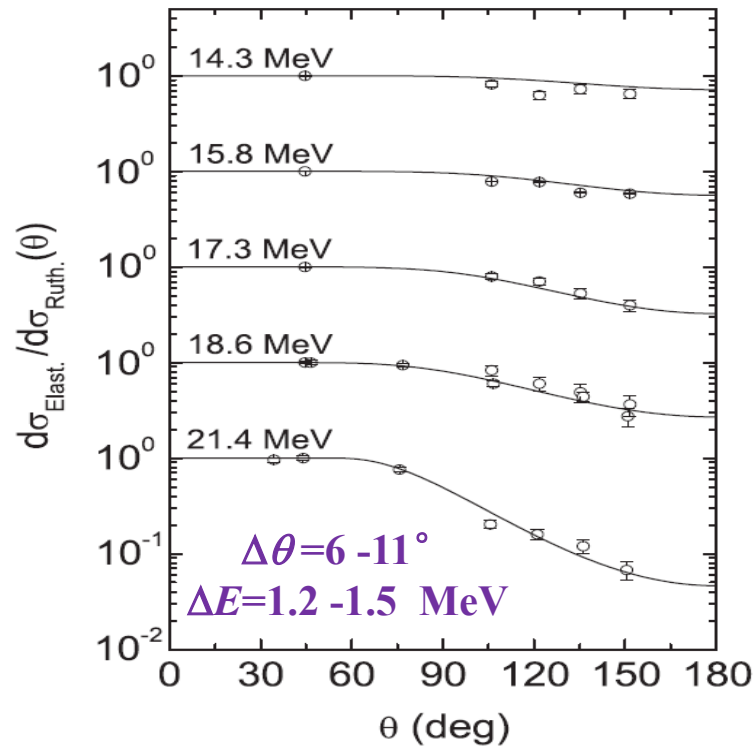


N. Keeley et al., Nucl. Phys. A **571**, 326 (1994).

Halo-nuclei Systems

Abnormal Threshold Anomaly

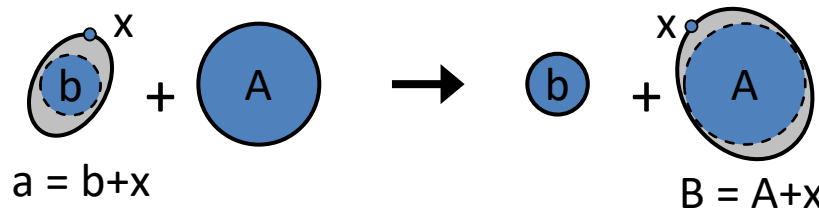
OMP's are usually extracted from elastic scattering.



★ Almost Impossible to extract effective OMP's at energy far below the barrier.

Cf: 1) E.F. Aguilera *et al.*, PRL **84**, 5058 (2000); PRC **63**, 061603R (2001).
2) A. R. Garcia *et al.*, Phys. Rev. C **76**, 067603 (2007).

Transfer Method



Transfer reaction $A(a,b)B$

$$\left(\frac{d\sigma}{d\Omega}\right)_{if} = P_{if} \left(\underbrace{\left(\frac{d\sigma}{d\Omega}\right)_{ii}}_{\text{elastic scattering}} \cdot \underbrace{\left(\frac{d\sigma}{d\Omega}\right)_{ff}}_{\text{cross sections}} \right)^{1/2}$$

elastic scattering cross sections

Transition amplitude: $T = J \int d^3r_b \int d^3r_a \chi^{(-)}(\vec{k}_f, \vec{r}_b)^* \langle bB|V|aA \rangle \chi^{(+)}(\vec{k}_i, \vec{r}_a)$,

4 wave functions are needed,

- ♣ two bound states: $b+x$ & $A+x$ (single-particle potential model)
- ♣ two scattering states: incoming & outgoing (optical potentials)

Proposed: C. J. Lin et al., AIP Conf. Proc. **853**, 81 (2006), presented at the FUSION06.

$^{16}\text{O}(^{14}\text{N}, ^{13}\text{C})^{17}\text{F}$: Chin. Phys. Lett. **25**, 4237 (2008).

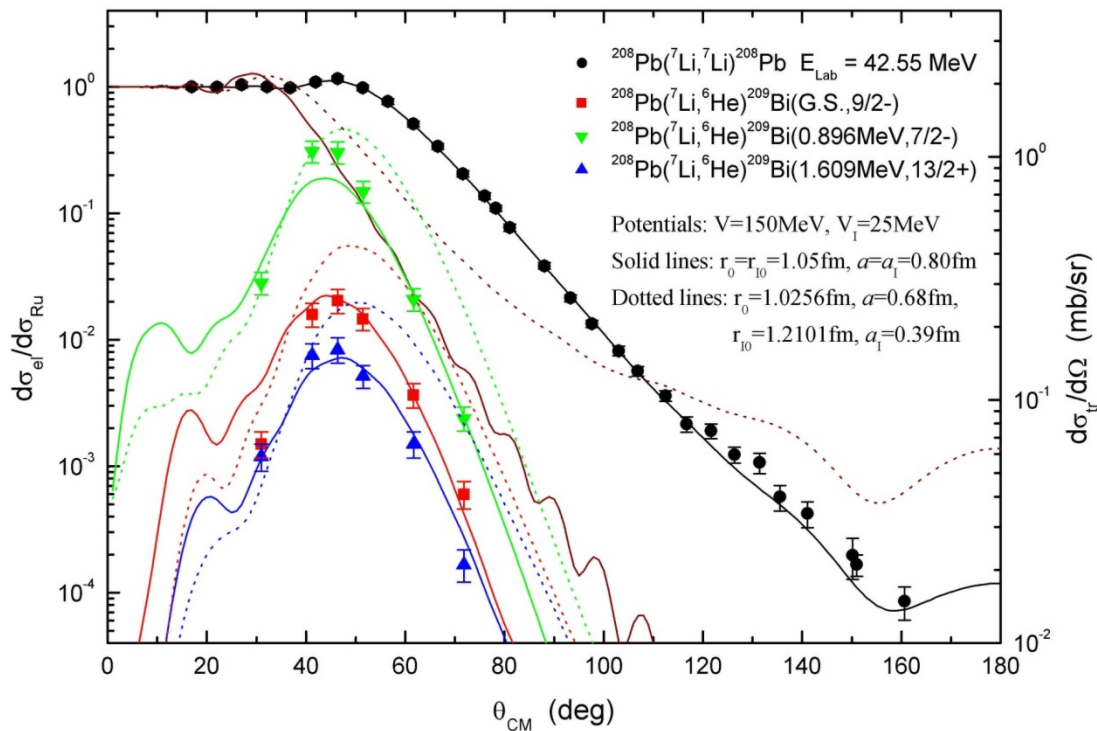
$^{11}\text{B}(^7\text{Li}, ^6\text{He})^{12}\text{C}$: Chin. Phys. Lett. **26**, 022503 (2009). Phys. Rev. C **87**, 047601 (2013).

$^{208}\text{Pb}(^7\text{Li}, ^6\text{He})^{209}\text{Bi}$: Phys. Rev. C **89**, 044615 (2014), Il Nuovo Cimento C **39**, 367 (2016), Chin. Phys. Lett. **31**, 092401 (2014), Phys. Rev. C **96**, 044615 (2017), Phys. Rev. Lett. **119**, 042503 (2017).

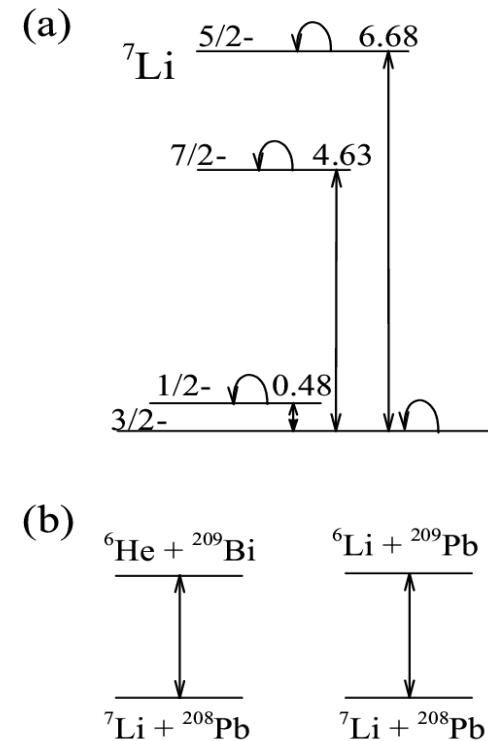
$^{63}\text{Cu}(^7\text{Li}, ^6\text{He})^{64}\text{Zn}$: Phys. Rev. C **95**, 034616 (2017).

Data Analysis: $^{208}\text{Pb}(^7\text{Li}, ^6\text{He})^{209}\text{Bi}$

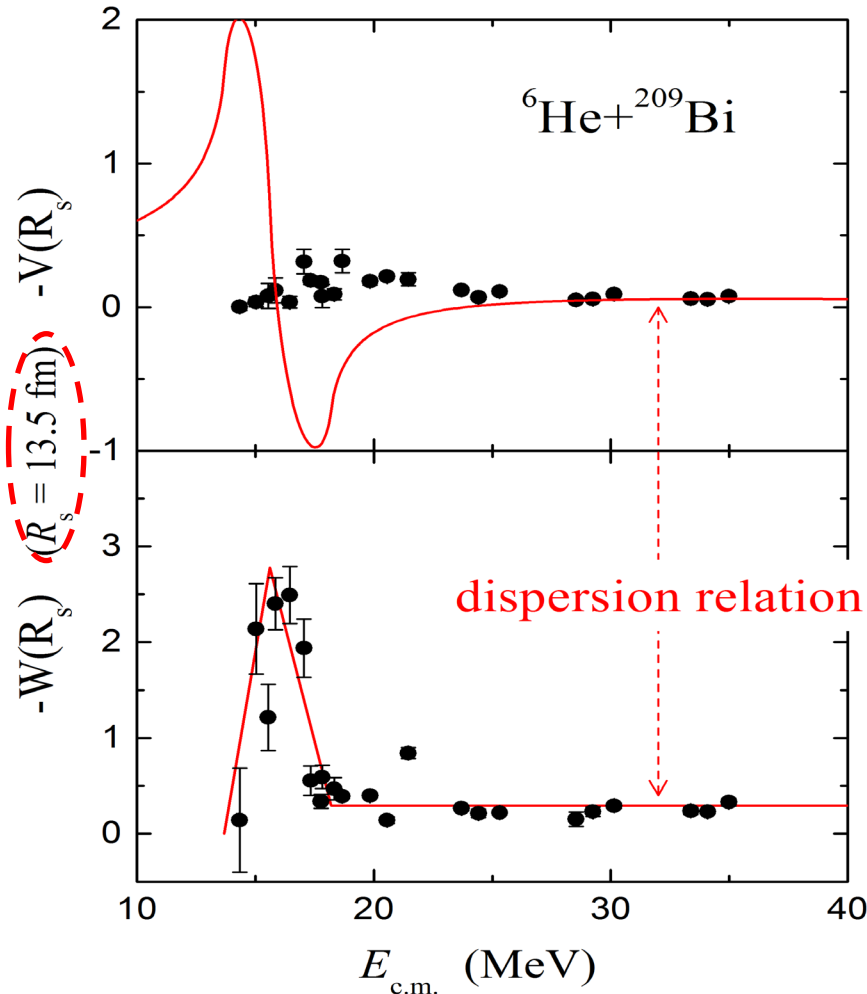
- Fit the elastic scattering to get the OP of $^7\text{Li}+^{208}\text{Pb}$
- Fit the transfer reactions to extract the OP of $^6\text{He}+^{209}\text{Bi}$
- By DWBA and CRC methods.



CRC scheme



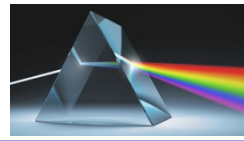
Results: $^{208}\text{Pb}(^7\text{Li}, ^6\text{He})^{209}\text{Bi}$



- ★ OMPs of the $^6\text{He}+^{209}\text{Bi}$ system are determined precisely for the first time;
- ★ The **decreasing trend** in the imaginary part is observed, and the **threshold energy** is about 13.73 MeV ($\sim 0.7V_B$);
- ★ The behavior of real part looks normal, i.e. like a bell shape around the barrier;
- ★ The dispersion relation **does NOT hold** in this system.

L. Yang, C.J. Lin, H.M. Jia et al., Phys. Rev. Lett. **119**, 042503 (2017);
Phys. Rev. C **96**, 044615 (2017).

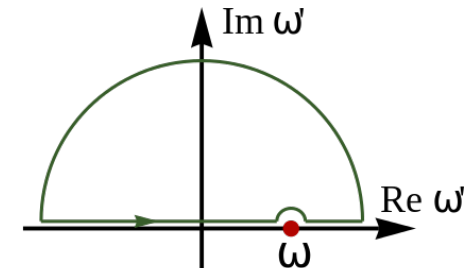
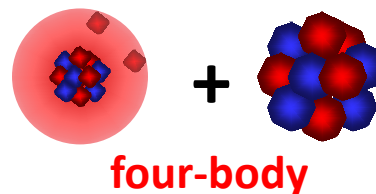
Discussions



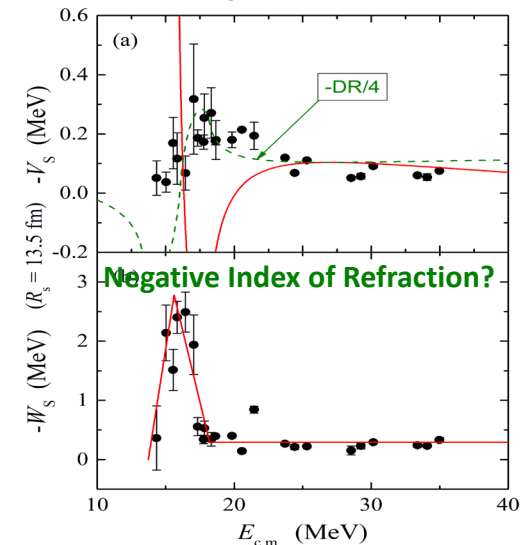
- ★ Dispersion relation results from causality, connecting real and imaginary part;
- ★ Any wave/particle should follow this rule when it passes through a media;
- ★ The classical dispersion relation is **not** applicable for exotic nuclear systems.

Possible reasons:

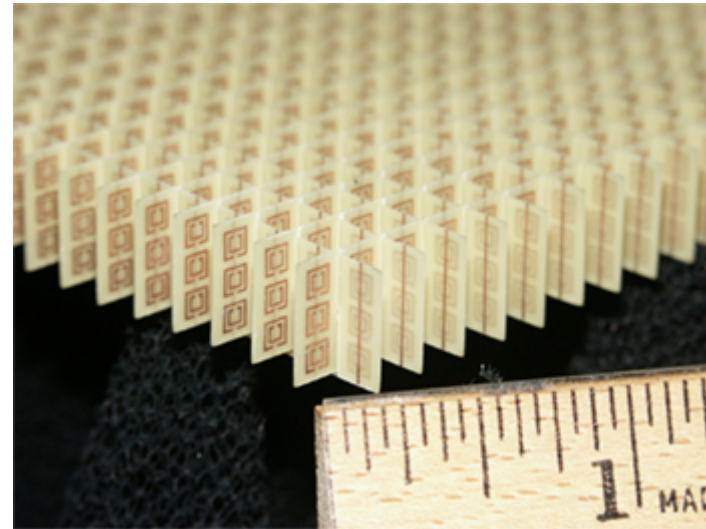
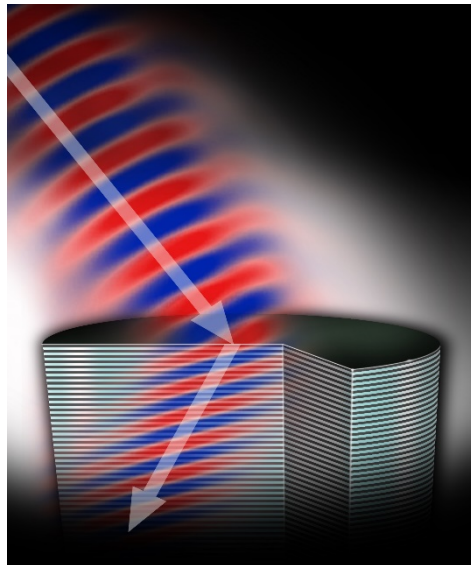
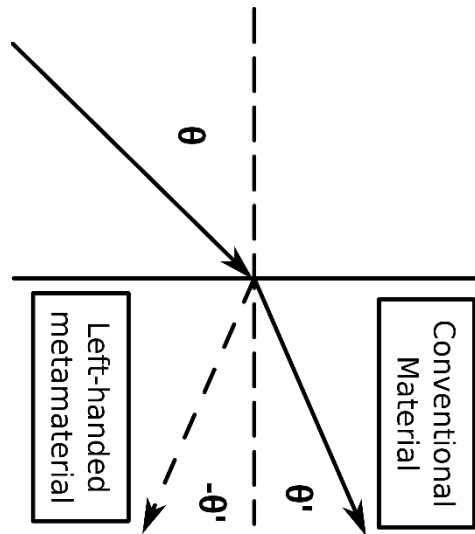
- **Causality** → dispersion relation
stable systems: causality ↔ analyticity
[Phys. Rev. **104**, 1760 (1956).]
- **Cauchy integration**
infinity poles (breakup) & off-axis (multi-process)
[Nucl. Phys. A **449**, 354 (1986).]
- **Negative Index of Refraction**
causality based criteria must be used with care
[Phys. Rev. Lett. **101**, 167401 (2008).]
- **Locality vs. non-locality**
equivalent local potential in Schrödinger equation



Cauchy's residue theorem



Negative Index Metamaterial

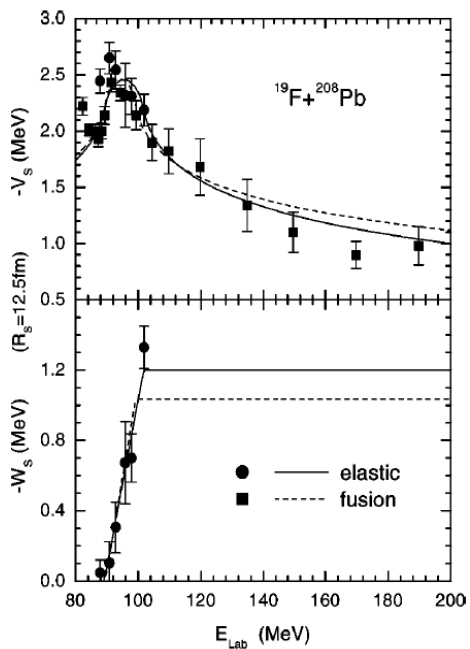


R.A. Shelby, D.R. Smith, S. Schultz, "Experimental Verification of a Negative Index of Refraction", *Science* **292**, 77 (2001).

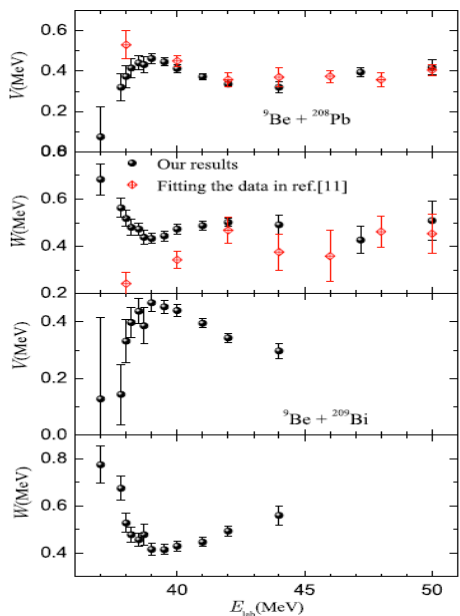
Negative refractive index metamaterials offer the possibility of revolutionary applications, such as subwavelength focusing [1], **invisibility cloaking** [2], and "trapped rainbow" **stopping of light** [3].

PRL **105**, 127401 (2010).

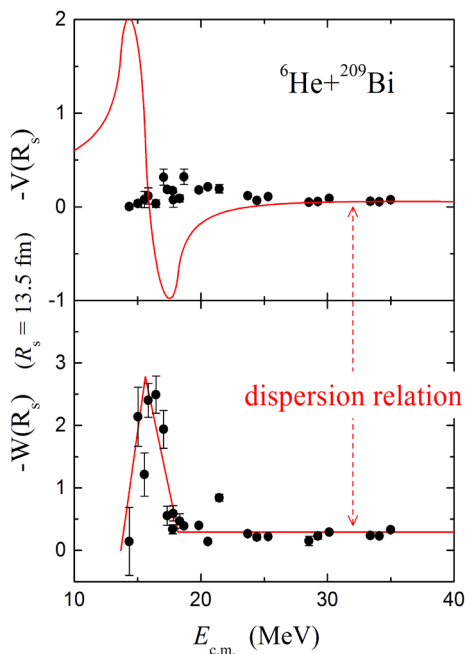
$^{17}\text{F}+^{208}\text{Pb}$



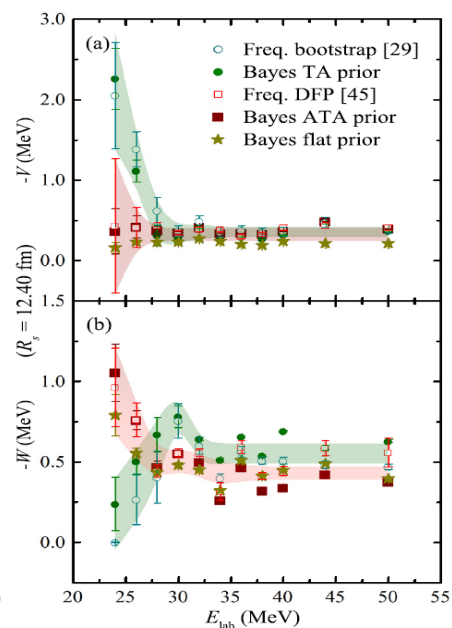
$^9\text{Be}+^{208}\text{Pb}, ^{209}\text{Bi}$



$^6\text{He}+^{209}\text{Bi}$



Bayes analyses



C.J. Lin et al.,
PRC **63**, 064606 (2001).

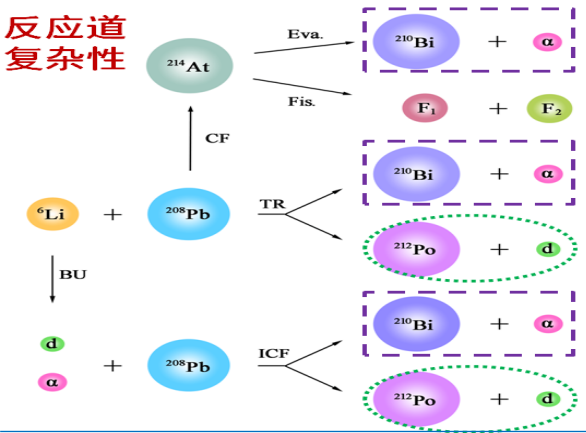
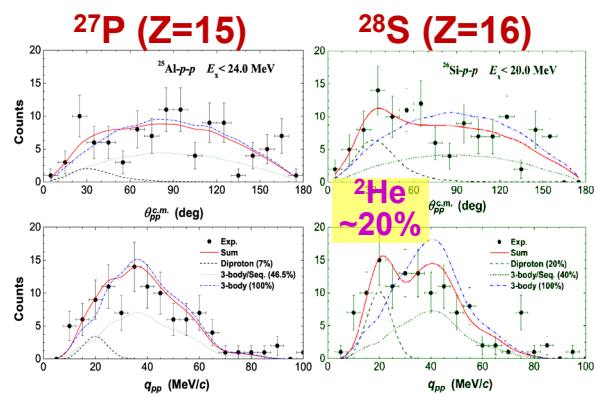
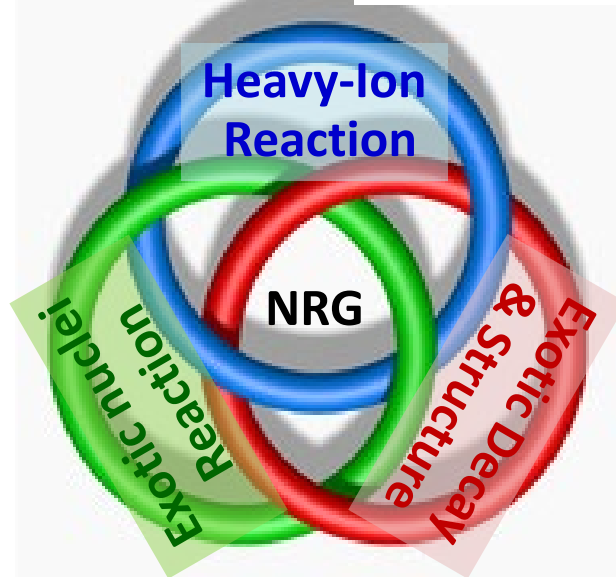
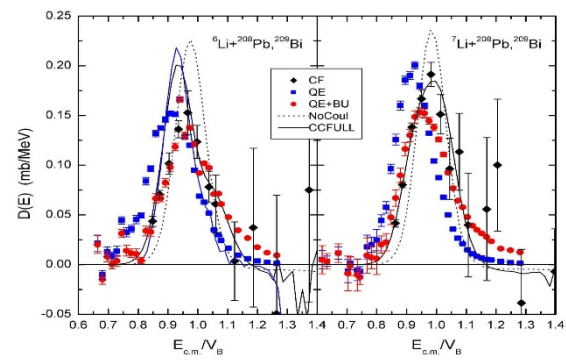
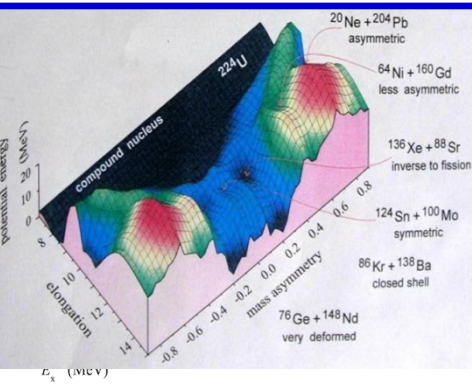
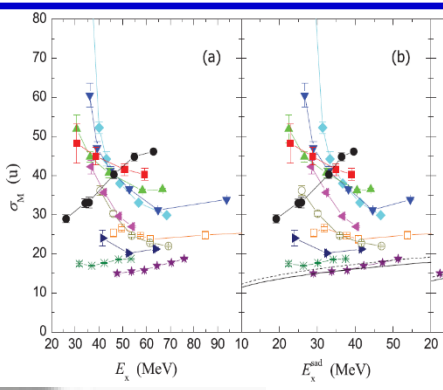
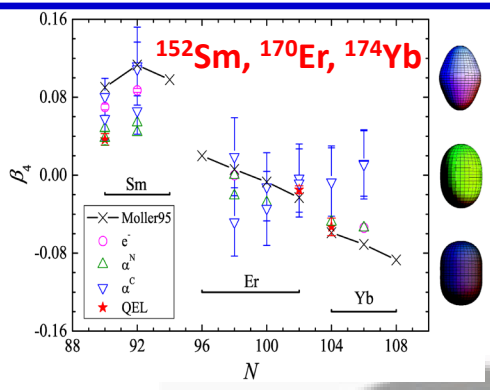
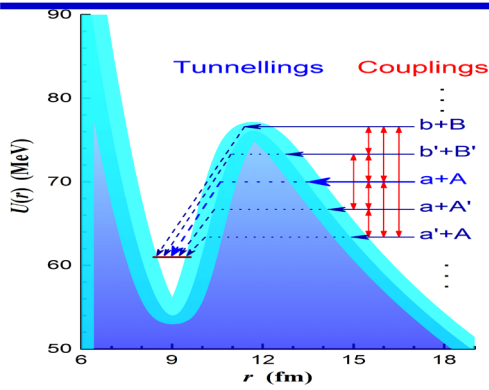
N. Yu et al.,
JPG **371**, 075108 (2010).

L. Yang et al.,
PRL **119**, 042503 (2017).

L. Yang et al.,
PLB **119**, 042503 (2020).

★ 紧束缚核体系：阈异常，色散关系 ← 因果关系；

★ 弱束缚核体系：反常阈异常，色散关系不成立。



代表性文章:
 Phys. Lett. B **813**, 136045 (2021).
 Phys. Rev. Lett. **125**, 192503 (2020).
 Phys. Lett. B **807**, 135540 (2020).
 Phys. Rev. Lett. **119**, 042503 (2017).
 Phys. Lett. B **766**, 312 (2017).

